

# Decentralized Optimization over Time-Varying Row-Stochastic Digraphs

Liyuan Liang\*      Yilong Song†      Kun Yuan‡

February 24, 2026

## Abstract

Decentralized optimization over directed graphs is essential for applications such as robotic swarms, sensor networks, and distributed learning. In many practical scenarios, the underlying network takes the form of a *Time-Varying Broadcast Network* (TVBN), where only row-stochastic mixing matrices can be constructed due to the unavailability of out-degree information. Achieving exact convergence for decentralized optimization over TVBNs has remained a long-standing open problem, as the limiting distribution of time-varying row-stochastic mixing matrices depends on unpredictable future graph realizations, rendering standard bias-correction techniques infeasible. This paper develops the first decentralized optimization algorithm that achieves exact convergence using only time-varying row-stochastic matrices. We first propose PULM (Pull-with-Memory), a gossip protocol that achieves average consensus with exponential convergence by alternating between row-stochastic mixing and local adjustment steps. Building on PULM, we develop PULM-DGD, which converges to a stationary solution at a rate of  $\mathcal{O}(\ln(T)/T)$  for smooth nonconvex objectives, where  $T$  denotes the communication round. Our results significantly broaden the applicability of decentralized optimization to highly dynamic communication environments.

## 1 Introduction

This paper investigates decentralized optimization over a network of  $n$  nodes:

$$\min_{x \in \mathbb{R}^d} f(x) := \frac{1}{n} \sum_{i=1}^n f_i(x). \quad (1)$$

Each objective function  $f_i$  is accessible only by node  $i$  and is assumed to be smooth and potentially nonconvex. The local losses  $f_i$  generally differ from each other, which poses challenges to both the design and analysis of distributed algorithms.

---

\*Equal contribution. Liyuan Liang is with School of Mathematics Science, Peking University (liangliyuaangg@gmail.com),

†Equal contribution. Yilong Song is with Academy for Advanced Interdisciplinary Studies, Peking University (2301213059@pku.edu.cn)

‡Corresponding author. Kun Yuan is with Center for Machine Learning Research, Peking University (kunyuan@pku.edu.cn)

Decentralized optimization eliminates the need for a central server, thereby enhancing flexibility and enabling broad applicability in peer-to-peer communication scenarios. As a result, the design of decentralized optimization algorithms is inherently shaped by the underlying communication network among nodes, which is typically modeled as a graph or characterized by a mixing matrix. This study focuses on decentralized optimization over *directed graphs*, or digraphs. Directed communication naturally models numerous real-world scenarios, including robotic swarms with asymmetric linkages [1, 2], sensor networks with unidirectional message transmission [3, 4], and distributed deep learning systems where bandwidth asymmetry constrains communication [5, 6].

## 1.1 Time-Varying Broadcast Network

The need for distributed optimization over directed graphs arises from complex communication constraints in real-world scenarios. Depending on the nature of these constraints, the underlying digraph may exhibit various challenging properties, including (1) not being symmetric, (2) having a time-varying topology, and (3) nodes lacking knowledge of their own out-degrees. In the most demanding communication settings, all three properties must be addressed simultaneously. We refer to a network exhibiting all these characteristics as a *Time-Varying Broadcast Network* (TVBN). In many practical applications, the communication setting can only be accurately modeled as a TVBN:

**Example 1** (Random Radio Broadcast). *In radio communications, transmitted information is received by any node within broadcast range, and the sender has no knowledge of which nodes have received the message. The network topology varies over time as nodes enter or exit the broadcast range.*

**Example 2** (Byzantine Attack). *A Byzantine attack occurs when a subset of agents in the system behaves maliciously or transmits corrupted information to other nodes. Nodes receiving such malicious information may attempt to ignore or discard these unreliable signals, resulting in a TVBN.*

**Example 3** (Packet Loss and Network Failure). *When packet loss or network failure occurs, receivers obtain incomplete or corrupted messages, creating uncertainty regarding the status of message delivery. Such scenarios can be modeled as a TVBN.*

While decentralized optimization over time-varying digraphs has been extensively studied, all existing results, to our knowledge, require nodes to be aware of their out-degrees. Building upon the push-sum protocol, seminal works [7, 8, 9] investigate decentralized algorithms over time-varying column-stochastic networks. To ensure column-stochastic mixing matrices, each node must know its out-degree, which is not feasible in highly dynamic communication environments. Even if a node correctly determines its out-degree and scales the mixing weights accordingly for its neighbors, a network failure occurring after transmission (but before reception) may prevent some neighbors from receiving the message. In this case, the effective out-degree changes unexpectedly, and column-stochasticity can no longer be guaranteed; see Figure 1 for an

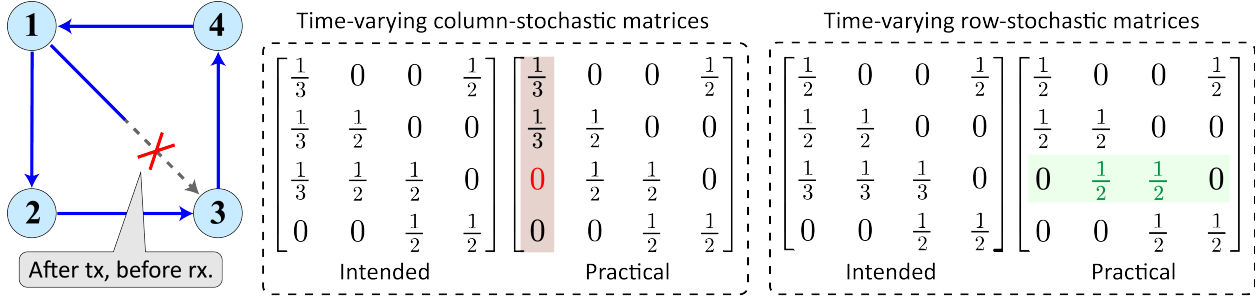


Figure 1: Left: A time-varying network with  $n = 4$  nodes experiencing unexpected network failure; “tx” and “rx” denote “transmission” and “reception,” respectively. Middle and right: The corresponding column- and row-stochastic mixing matrices. The network failure results in an incorrect column-stochastic matrix due to sudden changes in out-degree information. However, a correct row-stochastic matrix can still be constructed since it relies only on in-degree information (i.e., the actually received messages), which remains accessible.

illustration. Another important line of work [10, 11, 12] studies push-pull or AB algorithms over time-varying digraphs. Since these methods alternately rely on row-stochastic and column-stochastic matrices, they also require out-degree knowledge. In fact, *only algorithms relying purely on row-stochastic mixing matrices are feasible in TVBNs*, since each node only needs to know its in-degree, which is naturally immune to highly dynamic communication environments; see Figure 1 for an illustration.

## 1.2 Open Questions and Challenges

Decentralized optimization over time-varying column-stochastic digraphs is now well understood, with foundational methods [7, 13, 8] developed over a decade ago and subsequently extended by [9, 10]. However, developing algorithms that exactly solve problem (1) over purely time-varying row-stochastic digraphs (i.e., TVBNs) remains a long-standing open question.

Since the out-degree is inaccessible in TVBNs, even developing decentralized algorithms to achieve average consensus is challenging. Assume each node  $i \in [n]$  in the network initializes a vector  $x_i$ . Traditional gossip algorithms [14, 15] can only achieve consensus among nodes in TVBNs, but not average consensus  $n^{-1} \sum_{i=1}^n x_i$ . The approach most related to our setting is that of [16], which proposes a pre-correction strategy for *static* row-stochastic mixing matrices. This strategy exploits the following property: for a nonnegative row-stochastic matrix  $A$  with strong connectivity, there exists a unique Perron vector  $\pi_A$  (i.e.,  $\pi_A > 0$ ,  $\pi_A^\top A = \pi_A^\top$ ,  $\mathbf{1}_n^\top \pi_A = 1$ ) satisfying

$$A^k \rightarrow \mathbf{1}_n \pi_A^\top, \quad k \rightarrow \infty.$$

Using this property, [16] initializes  $z_i^{(0)} = (n[\pi_A]_i)^{-1} x_i$  at each node and iteratively propagate  $z_i$  over the network (which is equivalent to left-multiplying by  $A$ ):

$$\mathbf{z}^{(k)} = A^k \text{Diag}(\mathbf{1}_n^\top A^k)^{-1} \mathbf{x} \rightarrow \mathbf{1}_n \pi_A^\top \text{Diag}(n \pi_A)^{-1} \mathbf{x} = n^{-1} \mathbf{1}_n \mathbf{1}_n^\top \mathbf{x}, \quad k \rightarrow \infty \quad (2)$$

where we let  $\mathbf{z}^{(k)} := [(z_1^{(k)})^\top; (z_2^{(k)})^\top; \dots; (z_n^{(k)})^\top]$  and  $\mathbf{x} := [x_1^\top; x_2^\top; \dots; x_n^\top]$ .

However, the pre-correction strategy in (2) is inherently an offline, two-stage method. To form the corrected initialization  $z_i^{(0)} = (n[\pi_A]_i)^{-1}x_i$ , each agent must know the Perron vector  $\pi_A$  which is a *global* property of the static mixing matrix  $A$  and is not available locally in general; consequently, one must first run an auxiliary protocol to estimate  $\pi_A$  by repeated multiplication of  $A$ , and only then restart and run the main gossip iteration  $\mathbf{z}^{(k)} = A^k \text{Diag}(n\pi_A)^{-1}\mathbf{x}$  to obtain exact averaging<sup>1</sup>. Such a two-stage offline method fundamentally fails in the TVBN setting with time-varying  $A^{(k)}$ . Even if the first stage could estimate a Perron vector  $\pi_k = \pi(\{A^{(t)}\}_{t \leq k})$ , where the notation  $\pi(\cdot)$  represents a certain mapping, this estimate is only valid for the network state during stage one. When the second stage begins—applying the correction  $(n[\pi_k]_i)^{-1}x_i$  and running the gossip algorithm—the mixing matrices  $A^{(k+1)}, A^{(k+2)}, \dots$  continue to evolve, making the stage-one estimate of  $\pi_k$  immediately outdated. Since the Perron vector itself is non-stationary, there exists *no single fixed*  $\pi$  that can be estimated in stage one and remain valid throughout stage two.

### 1.3 Related Work

In connected networks, the topology is characterized by a mixing matrix. For undirected networks, constructing symmetric and *doubly stochastic* mixing matrices is straightforward. Early decentralized algorithms for such settings include decentralized gradient descent (DGD) [17], diffusion [18], and dual averaging [19]. These methods, however, exhibit bias under data heterogeneity [20]. To address this limitation, advanced algorithms have been developed based on explicit bias-correction [21, 22, 23] and gradient tracking [24, 25, 9, 26]. Extending these algorithms to time-varying undirected networks [9, 27] is natural, as time-varying doubly stochastic mixing matrices readily preserve essential average consensus properties.

For directed networks, constructing doubly stochastic matrices is generally infeasible. When the out-degree of each node is accessible, column-stochastic mixing matrices can be constructed [7, 28]. Decentralized algorithms using such column-stochastic matrices are well studied. They leverage the push-sum technique [29, 28] to correct the bias in column-stochastic communications and achieve global averaging of variables or gradients. While the subgradient-push algorithm [7, 28] guarantees convergence to optimality, its sublinear rate persists even under strong convexity. Subsequent work—including EXTRA-push [30], D-EXTRA [31], ADD-OPT [32], and Push-DIGing [9]—has achieved faster convergence by explicitly mitigating heterogeneity. Recent work [33] has established lower bounds and optimal algorithms for decentralized optimization over column-stochastic digraphs. Since the push-sum technique naturally accommodates time-varying column-stochastic digraphs, all the aforementioned algorithms readily extend to such settings.

When only in-degree information is available, one can construct row-stochastic mixing matrices. Diffusion [18, 34] was among the earliest decentralized algorithms using row-stochastic mixing matrices, but converges only to a Pareto-optimal solution rather than the global optimum. Just as push-sum underpins

---

<sup>1</sup>Strategy (2) cannot be implemented in a decentralized online manner. Although one could track  $V^{(k)} = AV^{(k-1)}$  with  $V^{(0)} = I$ , the update  $\mathbf{z}^{(k)} = V^{(k)}\mathbf{b}$  (where  $\mathbf{b} = \text{Diag}(\mathbf{1}_n^\top V^{(k)})^{-1}\mathbf{x}$ ) is not decentralized: the matrix  $V^{(k)}$  is typically much denser than  $A$ , requiring global communication.

column-stochastic algorithms, the pull-diaq gossip protocol [16] serves as an effective technique to correct the bias caused by row-stochastic communications. Reference [35] first adapted distributed gradient descent to this setting. Subsequently, gradient tracking techniques were extended to the row-stochastic scenario by [36, 37, 38], while momentum-based variants were developed in [39, 40]. However, all of these algorithms are designed exclusively for static row-stochastic digraphs. To the best of our knowledge, no existing algorithm can achieve exact convergence to the solution of problem (1) using purely row-stochastic mixing matrices due to the challenges discussed in Section 1.2.

In digraphs where both in-degree and out-degree information are available, the Push-Pull/AB methods [41, 42, 43, 44] can solve problem (1) by alternately using column-stochastic and row-stochastic mixing matrices [45, 46]. These algorithms typically achieve faster convergence than methods relying solely on column- or row-stochastic matrices and can handle both static and time-varying scenarios. However, they require knowledge of the out-degree at each node, which is unavailable in TVBNs.

## 1.4 Main Results

This paper develops the first algorithm to achieve exact convergence for problem (1) using only time-varying row-stochastic mixing matrices, thereby making decentralized optimization feasible over TVBNs and significantly enhancing its robustness to highly dynamic environments. Our results are:

- C1. **Effective average consensus protocol.** We propose PULL-with-Memory (**PULM**), a decentralized method to achieve average consensus over TVBNs with time-varying row-stochastic mixing matrices. By alternating between a standard row-stochastic gossip step and a local adjustment step, we theoretically prove that PULM converges to average consensus exponentially fast.
- C2. **The first exactly converging algorithm.** Built upon PULM, we develop a decentralized gradient descent approach over TVBNs, termed **PULM-DGD**. For nonconvex and smooth optimization problems, we establish that PULM-DGD converges to a stationary solution at a rate of  $\mathcal{O}(\frac{\ln(T)}{T})$ . To our best knowledge, PULM-DGD is the first method that achieves exact convergence using only time-varying row-stochastic mixing matrices.

**Organization.** The remainder of this paper is organized as follows. Notation and assumptions are provided in Section 2. In Section 3, we examine the mixing dynamics in TVBNs and derive our PULM approach for achieving distributed average consensus. Performing decentralized optimization through PULM is discussed in Section 4, where we provide the main convergence theorems. We conduct numerical experiments to verify PULM and PULM-DGD in Section 5 and conclude in Section 6.

## 2 Notations and Assumptions

In this section, we declare necessary notations and assumptions.

**Notations.** Let  $\mathbf{1}_n$  denote the vector of all-ones of  $n$  dimensions and  $I_n \in \mathbb{R}^{n \times n}$  the identity matrix. In the context of proofs, the notation  $E_n := \frac{1}{n} \mathbf{1}_n \mathbf{1}_n^\top$  is introduced for simplicity. We use  $[n]$  to denote the set  $\{1, 2, \dots, n\}$ . For a given vector  $v$  or a given matrix  $X$ ,  $\text{Diag}(v), \text{Diag}(X)$  signify the diagonal matrix whose diagonal elements are comprised of all the entries of  $v$ , or the diagonal elements of given  $X$ , respectively. We define  $n \times d$  matrices

$$\begin{aligned} \mathbf{x}^{(k)} &:= [(x_1^{(k)})^\top; (x_2^{(k)})^\top; \dots; (x_n^{(k)})^\top] \\ \mathbf{g}^{(k)} = \nabla F(\mathbf{x}^{(k)}) &:= [\nabla f_1(x_1^{(k)})^\top; \dots; \nabla f_n(x_n^{(k)})^\top] \end{aligned}$$

by stacking all local variables vertically. The upright bold symbols (e.g.  $\mathbf{x}, \mathbf{g}$ ) always denote network-level quantities. For vectors or matrices, we use the symbols  $\leq$  and  $\geq$  for element-wise comparison. We use  $\|\cdot\|$  for  $\ell_2$  vector norm and  $\|\cdot\|_F$  for matrix Frobenius norm. We use  $\|\cdot\|_2$  for induced  $\ell_2$  matrix norm, which means  $\|A\|_2 := \max_{\|v\|=1} \|Av\|$ . We use  $\max |A|$  to represent the maximum absolute value of all the elements of matrix  $A$ . Unless otherwise specified, product signs for matrices always indicate consecutive left multiplication in order, i.e.,  $\prod_{k=1}^K A^{(i)} := A^{(K)} A^{(K-1)} \dots A^{(2)} A^{(1)}$ . When a directed graph  $\mathcal{G}$  is classified as strongly connected, it means there exists a directed path from  $i$  to  $j$  for any nodes  $i, j$  in  $\mathcal{G}$ .

**Gossip communication.** When node  $i$  collects information  $x_j \in \mathbb{R}^d, j \in N_i^{\text{in}}$  from its in-neighbors, it can mix these vectors using scalars  $a_{ij}$ , producing  $x_i^{\text{new}} = \sum_{j \in N_i^{\text{in}}} a_{ij} x_j$ . This process is called gossip communication. Using the stacked notation  $\mathbf{x} = [x_1^\top; x_2^\top; \dots; x_n^\top]$  and  $A = [a_{ij}]_{n \times n}$ , the update can be written as  $\mathbf{x}^{\text{new}} \leftarrow A\mathbf{x}$ , where  $A$  is called the mixing matrix. When out-degrees are accessible,  $A$  can be constructed as either column-stochastic or row-stochastic. When out-degrees are inaccessible,  $A$  can only be row-stochastic.

**Assumptions.** The following assumptions are used throughout this paper.

**Assumption 1** ( $\tilde{B}$ -STRONGLY CONNECTED GRAPH SEQUENCE). *The time-varying directed graph sequence  $\{\mathcal{G}^{(k)} = (\mathcal{V}, \mathcal{E}^{(k)})\}_{k \geq 0}$  satisfies the following: there exists an integer  $\tilde{B} > 0$  such that for any  $k \geq 0$ , the  $\tilde{B}$ -step accumulated graph*

$$\mathcal{G}_k^{k+\tilde{B}-1} := \left( \mathcal{V}, \bigcup_{l=k}^{k+\tilde{B}-1} \mathcal{E}^{(l)} \right)$$

*is strongly connected. Additionally, each graph  $\mathcal{G}^{(k)}$  contains a self-loop at every node.*

**Assumption 2** (RAPIDLY CHANGING BROADCAST NETWORK). *For each  $k \geq 0$  and  $i \in [n]$ , node  $i$  does not know its out-degree  $d_i^{\text{out},(k)}$  in graph  $\mathcal{G}^{(k)}$ . Additionally, for each  $k \geq 0$ , the mixing matrix generated from  $\mathcal{G}^{(k)}$  can only be used once.*

The single-use constraint on mixing matrices in Assumption 2 reflects the rapidly changing topology: by the time communication using  $A^{(k)}$  completes, the network has already transitioned to  $\mathcal{G}^{(k+1)}$ , making  $A^{(k)}$  incompatible with the current network structure. This is typical in highly dynamic environments such as drone swarms.

**Definition 1** (COMPATIBLE MIXING MATRICES). A mixing matrix  $A = [a_{ij}]_{n \times n}$  is compatible with graph  $\mathcal{G}$  if  $a_{ij} > 0$  when  $(j \rightarrow i) \in \mathcal{E}$ , and  $a_{ij} = 0$  otherwise. Any compatible  $A$  for  $\mathcal{G}$  satisfying Assumption 2 is row-stochastic, i.e.,  $A\mathbf{1}_n = \mathbf{1}_n$ .

**Assumption 3** (LOWER BOUNDED ENTRIES). Suppose that for each  $k \geq 0$ , we have a mixing matrix  $A^{(k)}$  that is compatible with  $\mathcal{G}^{(k)}$ . There exists a scalar  $\tau > 0$  such that all nonzero entries of  $A^{(k)}$  satisfy  $a_{ij}^{(k)} \geq \tau$  for all  $k \geq 0$ .

Assumption 3 is naturally satisfied by setting  $A_{ij}^{(k)} = 1/d_i^{\text{in},(k)}$  and  $\tau = 1/n$ .

**Proposition 1.** For the sequence of time-varying directed graphs coupled with compatible mixing matrices  $\{\mathcal{G}^{(k)}, A^{(k)}\}_{k \geq 0}$  satisfying Assumptions 1–3, there exist an integer  $0 < B \leq n\tilde{B}$  and a scalar  $\eta \in [\tau^B, 1)$  such that  $\prod_{l=k}^{k+B-1} A^{(l)} \geq \eta, \forall k \geq 0$ .

Proposition 1 establishes that, for any starting time  $k$ , the  $B$ -step product of mixing matrices  $\prod_{l=k}^{k+B-1} A^{(l)}$  is entrywise lower bounded by a constant  $\eta > 0$ . This property is central to the convergence analysis: it implies uniform mixing over every  $B$ -step window, ensuring that each node’s information influences every other node with weight at least  $\eta$ , independent of  $k$ . The proof can be found in Appendix A.1. We next introduce our final assumption.

**Assumption 4** (SMOOTHNESS). All the local functions  $f_i(\cdot)$  are lower bounded, and there exists a constant  $L > 0$  such that for all  $i \in [n]$  and all  $x, y \in \mathbb{R}^d$ ,

$$\|\nabla f_i(x) - \nabla f_i(y)\| \leq L\|x - y\|.$$

### 3 Achieving Average Consensus over TVBNs

In this section, we analyze how information is mixed and propagated across TVBNs using time-varying row-stochastic mixing matrices only. To formalize this process, let each node  $i$  initialize a vector  $z_i^{(0)} = x_i$ . The  $k$ -th communication round is governed by the row-stochastic mixing matrix  $A^{(k)}$ . At the beginning of the  $k$ -th round, we assume each node  $i$  stores a vector  $z_i^{(k)}$ , which can be expressed as a linear combination of all initial vectors:

$$z_i^{(k)} = \sum_{j=1}^n w_{ij}^{(k)} x_j, \tag{3}$$

where  $\{w_{ij}^{(k)}\}$  are some weights to be determined later. Without loss of generality, we assume the initial vectors  $\{x_i\}_{i=1}^n$  are independent, which ensures that the coefficients  $\{w_{ij}^{(k)}\}$  are uniquely determined. We term process (3) the *mixing dynamics*.

### 3.1 Mixing Dynamics over TVBNs

By collecting coefficients  $w_{ij}^{(k)}$  in (3), we define the *distribution matrix*  $W^{(k)} := [w_{ij}^{(k)}]_{i,j=1}^n \in \mathbb{R}^{n \times n}$ , which maps the initial vectors  $\{x_j\}_{j=1}^n$  to the node states  $\{z_j^{(k)}\}_{j=1}^n$  at round  $k$ . In particular, letting  $\mathbf{z}^{(k)} := [z_1^{(k)}, \dots, z_n^{(k)}]^\top$  and  $\mathbf{x} := [x_1, \dots, x_n]^\top$ , the mixing dynamics (3) can be written compactly as  $\mathbf{z}^{(k)} = W^{(k)}\mathbf{x}$ . At initialization, each node stores its own vector  $z_i^{(0)} := x_i$ , hence  $W^{(0)} = I_n$ . Moreover, average consensus is achieved if  $W^{(k)} \rightarrow \frac{1}{n}\mathbf{1}_n\mathbf{1}_n^\top$  as  $k \rightarrow \infty$ . Using the mixing dynamics in (3), the gossip update  $z_i^{(k+1)} = \sum_{j=1}^n a_{ij}^{(k)} z_j^{(k)}$  is equivalent to performing the following matrix update

$$W^{(k+1)} = A^{(k)}W^{(k)}, \quad (4)$$

where  $A^{(k)} = [a_{ij}^{(k)}]_{n \times n}$  is row-stochastic. However, the simple gossip update (4) cannot drive  $W^{(k)}$  to  $n^{-1}\mathbf{1}_n\mathbf{1}_n^\top$ . Instead, it converges to a biased average:

**Proposition 2** (LIMITING PROPERTY). *For the sequence of time-varying directed graphs coupled with compatible mixing matrices  $\{\mathcal{G}^{(k)}, A^{(k)}\}_{k \geq 0}$  satisfying Assumptions 1–3, the infinite product  $\prod_{k=1}^{\infty} A^{(k)}$  converges, and the limit takes the form of  $\prod_{k=1}^{\infty} A^{(k)} = \mathbf{1}_n\pi^\top$ , where  $\pi = \pi(\{A^{(k)}\}_{k=0}^{\infty}) \in \mathbb{R}^n$ , which means that  $\pi$  is determined by the whole sequence  $\{A^{(k)}\}_{k=0}^{\infty}$ . Moreover, the convergence occurs at an exponential rate:*

$$\left\| \prod_{i=0}^{k-1} A^{(i)} - \mathbf{1}_n\pi^\top \right\|_F \leq n^{3/2} \frac{1+\eta}{\eta(1-\eta)} \cdot \left( \sqrt[B]{1-\eta} \right)^k, \quad (5)$$

where  $B$  and  $\eta$  are defined in Proposition 1.

*Proof.* See Appendix A.3. □

While Proposition 2 guarantees asymptotic consensus, the limit is a  $\pi$ -weighted average rather than the uniform average consensus  $n^{-1} \sum_{i=1}^n x_i$ . Moreover, the limit vector  $\pi$  cannot be exactly determined by the finite initial sequence  $\{A^{(l)}\}_{l=0}^{k-1}, \forall k < \infty$ . In fact, one can construct future sequence  $\{A^{(l)}\}_{l=k}^{\infty}$  arbitrarily that yields any desired limit vector  $\pi_k = \pi(\{A^{(l)}\}_{l=k}^{\infty})$ . The relation between the original limit and the limit induced by the tail sequence starting from the  $k$ -th matrix is given by

$$\mathbf{1}_n\pi^\top = \prod_{l=0}^{\infty} A^{(l)} = \prod_{l=k}^{\infty} A^{(l)} \prod_{l=0}^{k-1} A^{(l)} = \mathbf{1}_n\pi_k^\top \prod_{l=0}^{k-1} A^{(l)},$$

namely  $\pi^\top = \pi_k^\top \prod_{l=0}^{k-1} A^{(l)}$ . Given that  $\pi_k$  is arbitrary, the intended limit vector  $\pi$  is unpredictable if we only utilize the past observations of  $\{A^{(l)}\}_{l=0}^{k-1}$ . This poses a fundamental challenge for the two-stage offline pre-correction strategy (2).

The following remark further clarifies why average consensus can be achieved easily through time-varying column-stochastic mixing matrices, yet remains challenging when using time-varying row-stochastic mixing matrices.

**Remark 1** (COLUMN-STOCHASTIC VS ROW-STOCHASTIC MATRICES). *Average consensus is more easily achieved using column-stochastic mixing matrices. For a nonnegative column-stochastic matrix  $B$  with strong*

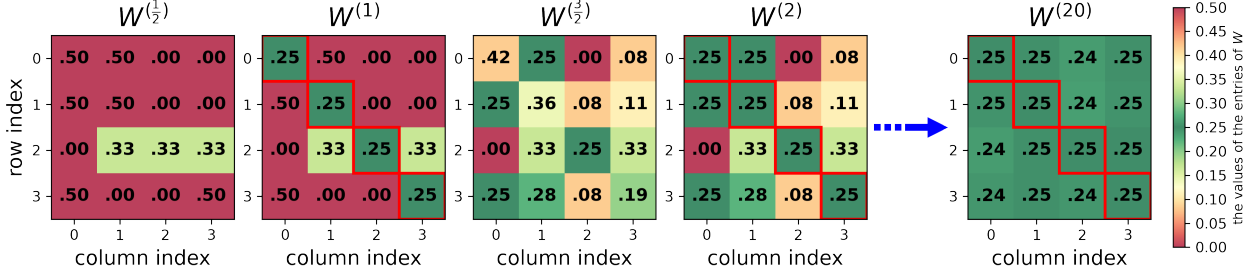


Figure 2: **Diffusion of the  $1/n$  diagonal anchor under the adjust-gossip update.** The adjust step anchors each diagonal entry  $w_{jj}$  at  $1/n$ ; the gossip step then diffuses this value down column  $j$ , pulling off-diagonal entries toward  $1/n$ . Cell colors indicate distance to  $1/n$  (greener means closer), showing how the anchored mass spreads from the diagonal throughout each column, driving  $W^{(k)}$  toward average consensus.

connectivity, there exists a unique Perron vector  $\pi_B$  (i.e.,  $\pi_B > 0$ ,  $B\pi_B = \pi_B$ ,  $\mathbf{1}_n^\top \pi_B = 1$ ) satisfying  $B^k \rightarrow \pi_B \mathbf{1}_n^\top$  as  $k \rightarrow \infty$ . The push-sum protocol [29, 28] achieves average consensus as follows

$$\mathbf{z}^{(k)} = \text{Diag}(B^k \mathbf{1}_n)^{-1} B^k \mathbf{x} \rightarrow \text{Diag}(n\pi_B)^{-1} \pi_B \mathbf{1}_n^\top \mathbf{x} = n^{-1} \mathbf{1}_n \mathbf{1}_n^\top \mathbf{x}, \quad k \rightarrow \infty. \quad (6)$$

In contrast to row-stochastic strategy (2), which applies pre-correction  $[\text{Diag}(n\pi)]^{-1}$  prior to gossip and requires knowledge of the limit vector  $\pi$  in advance, the column-stochastic approach (6) employs post-correction: nodes first propagate information via gossip, then apply local corrections. Crucially, this approach does not require prior knowledge of the limit vector  $\pi$ , thereby enabling an online single-stage implementation that naturally extends to time-varying scenarios. Specifically, by updating  $\mathbf{z}^{(k)} = B^{(k)} \mathbf{z}^{(k-1)}$  and  $v^{(k)} = B^{(k)} v^{(k-1)}$  with  $v^{(0)} = \mathbf{1}_n$ , each node obtains  $y_i^{(k)} = z_i^{(k)} / v_i^{(k)} \rightarrow n^{-1} \mathbf{1}_n^\top \mathbf{x}$  as  $k \rightarrow \infty$ . This distinction between pre-correction and post-correction explains why decentralized optimization over time-varying column-stochastic digraphs is well understood, while time-varying row-stochastic digraphs remains an open problem.

### 3.2 Shifting the Limits towards Average Consensus

Our method leverages a simple observation: since the limiting distribution  $\pi$  depends on the entire sequence of mixing matrices, judicious modifications of the intermediate  $W^{(k)}$  can steer  $\pi$  towards any desired value. Specifically, before left-multiplying by  $A^{(k)}$ , we introduce an adjustment step designed to shift the limiting vector closer to the average consensus. Through repeated adjustments, the process is progressively driven toward the desired average  $n^{-1} \mathbf{1}_n$ . This gossip-adjust process can be represented as:

$$\dots \rightarrow W^{(k)} \xrightarrow{A^{(k)}} W^{(k+\frac{1}{2})} \xrightarrow{\text{adjust}} W^{(k+1)} \xrightarrow{A^{(k+1)}} W^{(k+1+\frac{1}{2})} \xrightarrow{\text{adjust}} W^{(k+2)} \rightarrow \dots,$$

where  $\xrightarrow{A^{(k)}}$  denotes the gossip step and  $\xrightarrow{\text{adjust}}$  denotes the adjustment step. Crucially, this adjustment must be communication-free and rely on locally available information.

---

**Algorithm 1** Matrix-level procedure for driving  $W^{(k)}$  to  $n^{-1}\mathbf{1}_n\mathbf{1}_n^\top$ 


---

- 1: Initialize  $W^{(0)} = I_n$ .
  - 2: **for**  $k = 0, 1, 2, \dots, K - 1$  **do**
  - 3:      $W^{(k+\frac{1}{2})} = A^{(k)}W^{(k)}$ ;
  - 4:     Replace the diagonal entries of  $W^{(k+\frac{1}{2})}$  by  $\frac{1}{n}$ , and name it  $W^{(k+1)}$ ;
  - 5: **end for**
  - 6: **Output:**  $W^{(K)}$
- 

Algorithm 1 summarizes our proposed procedure. The intuition behind why it drives  $W^{(k)}$  toward  $n^{-1}\mathbf{1}_n\mathbf{1}_n^\top$  is straightforward: each iteration alternates between a *gossip* step, which computes  $W^{(k+\frac{1}{2})} = A^{(k)}W^{(k)}$  through convex combinations of rows of  $W$ , and an *adjust* step, which resets diagonal entries to  $1/n$ . Since gossip averages across rows (see (4)), entries within each column are repeatedly mixed, progressively converging to the same value (see Proposition 2). Since column  $j$  always contains the anchored value  $W_{jj}^{(k+1)} = 1/n$ , this mixing pulls off-diagonal entries toward  $1/n$ —effectively diffusing the anchor throughout the column (see Figure 2). Over successive iterations, all entries converge to  $1/n$ . We illustrate the performance of Algorithm 1 with a simple numerical simulation, demonstrating that the procedure converges exponentially fast to average consensus over various time-varying networks using row-stochastic matrices (see Figure 3).

### 3.3 The PULM Algorithm

We define  $D^{(k)} := \text{Diag}(A^{(k)}W^{(k)}) - I_n$ . The iteration of  $W^{(k)}$  in Algorithm 1 can be expressed as

$$W^{(k+\frac{1}{2})} = A^{(k)}W^{(k)}, \quad D^{(k)} = \text{Diag}(W^{(k+\frac{1}{2})}) - n^{-1}I_n, \quad W^{(k+1)} = W^{(k+\frac{1}{2})} - D^{(k)}.$$

If we let  $\mathbf{z}^{(k+1)} = W^{(k+1)}\mathbf{x}$ , then  $\mathbf{z}^{(k+1)} \rightarrow n^{-1}\mathbf{1}_n\mathbf{1}_n^\top\mathbf{x}$  based on the discussion in Section 3.2. While the above procedure can achieve average consensus with time-varying row-stochastic mixing matrices, it is not implemented in a decentralized manner, since  $W^{(k)}$  can be rather dense and may require global communication. To address this, we propose the following recursion of  $\mathbf{z}^{(k)}$ :

$$\mathbf{z}^{(k+\frac{1}{2})} = A^{(k)}\mathbf{z}^{(k)}, \quad \mathbf{z}^{(k+1)} = \mathbf{z}^{(k+\frac{1}{2})} - D^{(k)}\mathbf{x}. \quad (7)$$

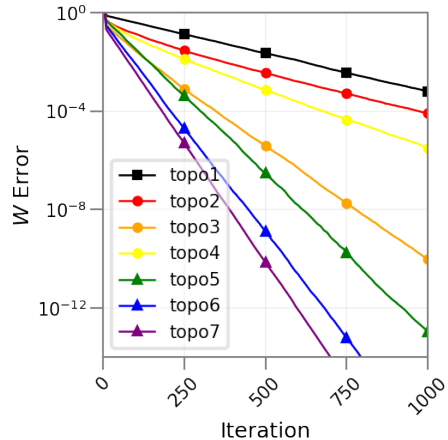


Figure 3: Convergence of  $W^{(k)}$ .  $W$  Error implies  $\|W^{(k)} - n^{-1}\mathbf{1}_n\mathbf{1}_n^\top\|_F$ . Details are in Appendix B.7.

---

**Algorithm 2** Pull with Memory (Node-wise implementation of Algorithm 1)

---

- 1: **Input:** Vector  $x_i \in \mathbb{R}^d$  at each node  $i \in [n]$  to be averaged
  - 2: **for** each node  $i \in [n]$  in parallel **do**
  - 3:     Initialize  $z_i^{(0)} = x_i$  and  $w_i^{(0)} = e_i$ , where  $e_i$  is the  $i$ -th column of  $I_n$
  - 4:     **for**  $k = 0, 1, 2, \dots, K - 1$  **do**
  - 5:         **Gossip:**  $z_i^{(k+\frac{1}{2})} = \sum_{j=1}^n a_{ij}^{(k)} z_j^{(k)}$  and  $w_i^{(k+\frac{1}{2})} = \sum_{j=1}^n a_{ij}^{(k)} w_j^{(k)}$
  - 6:         **Adjust:**  $d_i^{(k)} = [w_i^{(k+\frac{1}{2})}]_i - \frac{1}{n}$
  - 7:         **Update:**  $z_i^{(k+1)} = z_i^{(k+\frac{1}{2})} - d_i^{(k)} \cdot x_i$  and  $w_i^{(k+1)} = w_i^{(k+\frac{1}{2})} - d_i^{(k)} \cdot e_i$
  - 8:     **end for**
  - 9: **end for**
  - 10: **Output:**  $z_i^{(K)}$  at each node  $i \in [n]$
- 

We now show that  $\mathbf{z}^{(k+1)} = W^{(k+1)}\mathbf{x}$  using this recursion. Observe that

$$\begin{aligned} \mathbf{z}^{(k+1)} &= A^{(k)}\mathbf{z}^{(k)} - D^{(k)}\mathbf{x} = A^{(k)}\mathbf{z}^{(k)} - (A^{(k)}W^{(k)} - W^{(k+1)})\mathbf{x} \\ &= A^{(k)}\mathbf{z}^{(k)} - A^{(k)}W^{(k)}\mathbf{x} + W^{(k+1)}\mathbf{x}, \end{aligned}$$

which implies

$$\mathbf{z}^{(k+1)} - W^{(k+1)}\mathbf{x} = A^{(k)}(\mathbf{z}^{(k)} - W^{(k)}\mathbf{x}) = \prod_{i=0}^k A^{(i)}(\mathbf{z}^{(0)} - W^{(0)}\mathbf{x}) = 0. \quad (8)$$

where the last equation holds because we choose  $z_i^{(0)} = x_i$  and  $W^{(0)} = I_n$ . A decentralized implementation of recursion (7) is given by Algorithm 2. We name this algorithm PULM (Pull with Memory) because gossiping with a row-stochastic matrix is commonly referred to as a ‘‘pull’’ operation, and our method additionally requires each node to store and update its distribution vector  $w_i^{(k)}$ , which serves as a ‘‘memory’’ of the mixing process.

The following theorem establishes that PULM achieves monotonic and exponentially fast convergence.

**Theorem 1.** *For the sequence of time-varying directed graphs coupled with compatible mixing matrices  $\{\mathcal{G}^{(k)}, A^{(k)}\}_{k \geq 0}$  satisfying Assumptions 1–3, the following statements hold:*

- (i) *In Algorithm 1, the sequence  $\{\max_{i,j} |[W^{(k)}]_{ij} - n^{-1}|\}_{k \geq 0}$  is non-increasing.*
- (ii) *In both Algorithms 1 and 2,*

$$\|W^{(K)} - n^{-1}\mathbf{1}_n\mathbf{1}_n^\top\|_F \leq \frac{n}{1-\eta}(1-\eta)^{K/B}. \quad (9)$$

- (iii) *In Algorithm 2,*

$$\|\mathbf{z}^{(K)} - n^{-1}\mathbf{1}_n\mathbf{1}_n^\top\mathbf{x}\|_F \leq \frac{n}{1-\eta}(1-\eta)^{K/B}\|\mathbf{x}\|_F.$$

Here, the constants  $B > 0$  and  $\eta \in (0, 1)$  are defined in Proposition 1.

*Proof.* See Appendix A.5. □

## 4 Decentralized Optimization over TVBNs

While PULM is effective for achieving average consensus with time-varying row-stochastic matrices, it cannot directly solve the optimization problem (1). In this section, we extend PULM to address this setting.

### 4.1 Main recursion

A natural extension of PULM to decentralized optimization alternates between local gradient updates and a sufficiently long mixing phase:

$$\mathbf{x}^{(k+1)} = \text{PULM}(\mathbf{x}^{(k)} - \gamma \mathbf{g}^{(k)}, R_k), \quad (10)$$

where  $\text{PULM}(\mathbf{x}, R)$  denotes the output of Algorithm 2 after  $R$  iterations initialized at  $\mathbf{x}$ ,  $\gamma > 0$  is the step size, and  $\mathbf{g}^{(k)}$  denotes the stacked local gradients. When  $R_k$  is sufficiently large, the PULM stage effectively averages the post-gradient iterates, reducing (10) to the standard local-update-then-average scheme analogous to FedAvg [47]. Consequently, one might reasonably expect (10) to converge under standard assumptions.

Nevertheless, we do not adopt (10). Instead, we propose the following alternative:

$$\mathbf{x}^{(k+1)} = \text{Gossip}(\mathbf{x}^{(k)}, R_k) - \gamma \text{PULM}(\mathbf{g}^{(k)}, R_k), \quad (11)$$

where  $\text{Gossip}(\mathbf{x}^{(k)}, R_k) := \left(\prod_{r=0}^{R_k-1} A^{(k,r)}\right) \mathbf{x}^{(k)}$  and  $A^{(k,r)}$  denotes the row-stochastic mixing matrix at outer iteration  $k$  and inner iteration  $r$ . That is, standard gossip is applied to the parameter vector, while PULM is applied to the gradient vector.

### 4.2 Insight for parameter gossiping and gradient averaging

This distinction between mixing strategies reflects their differing roles: parameter mixing needs only to drive the iterates toward consensus, whereas gradient mixing critically requires a globally averaging mechanism to eliminate the non-uniform bias.

First, for the parameter trajectory, average consensus is unnecessary: we only need agents to agree on the same iterate, i.e.,  $\mathbf{x}^{(k)} \approx \mathbb{1}_n (x^{(k)})^\top$ . Naive Gossip directly contracts toward the consensus subspace under standard connectivity assumptions, and the weighted average it produces is acceptable for parameters. In contrast, PULM corrects this weighting bias to recover the exact global average—essential for gradients to drive unbiased descent. Moreover, for a fixed communication budget  $R_k$ , naive Gossip is more efficient, as PULM’s correction step slows disagreement contraction.

Second, Gossip preserves the consensus subspace exactly per iteration, whereas PULM does not necessarily preserve it at intermediate iterates due to its internal correction mechanism. Specifically, if  $\mathbf{x}^{(k)} = \mathbb{1}_n x^\top$ , then  $\left(\prod_{r=0}^{R_k-1} A^{(k,r)}\right) \mathbb{1}_n x^\top = \mathbb{1}_n x^\top \equiv \mathbf{x}^{(k)}$ , where we use  $A^{(k,r)} \mathbb{1}_n = \mathbb{1}_n$ . In contrast,  $\text{PULM}(\cdot, R_k)$  may perturb a consensual input before converging asymptotically to the average. Hence,  $\text{PULM}(\mathbf{x}^{(k)}, R_k) \neq \mathbf{x}^{(k)}$

---

**Algorithm 3** PULM-based Decentralized Gradient Descent (PULM-DGD)
 

---

- 1: **Input:** Step size  $\gamma > 0$ , inner iterations  $\{R_k\}_{k \geq 0}$
  - 2: **for** each node  $i \in [n]$  in parallel **do**
  - 3:   Initialize all variables to the same arbitrary value  $x_i^{(0)} = x^{(0)}$
  - 4:   **for**  $k = 0, 1, 2, \dots, K - 1$  **do**
  - 5:     Compute local gradient:  $g_i^{(k)} = \nabla f_i(x_i^{(k)})$
  - 6:     Initialize  $z_i^{(k,0)} = x_i^{(k)} - \gamma g_i^{(k)}$  and  $w_i^{(k,0)} = \mathbf{e}_i$
  - 7:     **for**  $r = 0, 1, 2, \dots, R_k - 1$  **do** ▷ PULM inner loop
  - 8:       **Gossip:**  $z_i^{(k,r+\frac{1}{2})} = \sum_{j=1}^n a_{ij}^{(k,r)} z_j^{(k,r)}$ ,  $w_i^{(k,r+\frac{1}{2})} = \sum_{j=1}^n a_{ij}^{(k,r)} w_j^{(k,r)}$
  - 9:       **Adjust:**  $d_i^{(k,r)} = [w_i^{(k,r+\frac{1}{2})}]_i - \frac{1}{n}$
  - 10:       **Update:**  $z_i^{(k,r+1)} = z_i^{(k,r+\frac{1}{2})} + \gamma d_i^{(k,r)} g_i^{(k)}$ ,  $w_i^{(k,r+1)} = w_i^{(k,r+\frac{1}{2})} - d_i^{(k,r)} \mathbf{e}_i$
  - 11:     **end for**
  - 12:      $x_i^{(k+1)} = z_i^{(k,R_k)}$
  - 13:   **end for**
  - 14: **end for**
  - 15: **Output:**  $x_i^{(K)}$  at each node  $i \in [n]$
- 

even when  $\mathbf{x}^{(k)}$  is consensual. Moreover, in our setting,  $\mathbf{x}^{(0)}$  is initialized as consensual, and each update increment  $\gamma \mathbf{g}^{(k)}$  is small due to the stepsize choice. Consequently, the iterates  $\mathbf{x}^{(k)}$  are typically already close to consensus at each stage, making it desirable for the communication operator to preserve this existing alignment. This invariance property makes Gossip the natural choice for parameters when already-aligned models should remain aligned throughout the communication phase.

### 4.3 PULM-DGD Method

The main recursion (11) involves  $R_k$  inner iterations. We now describe how to implement these inner iterations in a fully decentralized manner. Initialize  $\mathbf{z}^{(k,0)} = \mathbf{x}^{(k)} - \gamma \mathbf{g}^{(k)}$ , we first update  $W^{(k,r+1)}$  as in Section 3.3:

$$W^{(k,r+\frac{1}{2})} = A^{(k,r)} W^{(k,r)}, D^{(k,r)} = \text{Diag}(W^{(k,r+\frac{1}{2})}) - n^{-1} I_n, W^{(k,r+1)} = W^{(k,r+\frac{1}{2})} - D^{(k,r)}$$

for  $r = 0, 1, \dots, R_k - 1$ . Next, we propose PULM-DGD which updates  $\mathbf{z}^{(k,r+1)}$  as:

$$\mathbf{z}^{(k,r+1)} = A^{(k,r)} \mathbf{z}^{(k,r)} + \gamma D^{(k,r)} \mathbf{g}^{(k)}. \quad (12)$$

After  $R_k$  inner iterations, we set  $\mathbf{x}^{(k+1)} = \mathbf{z}^{(k,R_k)}$ . We now show that the above procedure is equivalent to the main recursion (11). Observe that

$$\begin{aligned} \mathbf{z}^{(k,r+1)} &= A^{(k,r)} \mathbf{z}^{(k,r)} + \gamma (A^{(k,r)} W^{(k,r)} - W^{(k,r+1)}) \mathbf{g}^{(k)} \\ &= A^{(k,r)} \mathbf{z}^{(k,r)} + \gamma A^{(k,r)} W^{(k,r)} \mathbf{g}^{(k)} - \gamma W^{(k,r+1)} \mathbf{g}^{(k)}, \end{aligned}$$

which implies

$$\mathbf{z}^{(k,r+1)} + \gamma W^{(k,r+1)} \mathbf{g}^{(k)} = A^{(k,r)} (\mathbf{z}^{(k,r)} + \gamma W^{(k,r)} \mathbf{g}^{(k)}).$$

Applying this relation recursively, we obtain

$$\mathbf{z}^{(k,R_k)} + \gamma W^{(k,R_k)} \mathbf{g}^{(k)} = \prod_{r=0}^{R_k-1} A^{(k,r)} (\mathbf{z}^{(k,0)} + \gamma W^{(k,0)} \mathbf{g}^{(k)}) = \prod_{r=0}^{R_k-1} A^{(k,r)} \mathbf{x}^{(k)},$$

where the last equality follows from  $W^{(k,0)} = I_n$  and  $\mathbf{z}^{(k,0)} = \mathbf{x}^{(k)} - \gamma \mathbf{g}^{(k)}$ . Thus,

$$\mathbf{x}^{(k+1)} = \mathbf{z}^{(k,R_k)} = \prod_{r=0}^{R_k-1} A^{(k,r)} \mathbf{x}^{(k)} - \gamma W^{(k,R_k)} \mathbf{g}^{(k)}, \quad (13)$$

which is precisely the main recursion (11). A decentralized implementation of PULM-DGD is presented in Algorithm 3.

#### 4.4 Convergence Analysis

To facilitate the convergence analysis, we introduce the following notation. Let  $\bar{g}^{(k)} := \frac{1}{n} \sum_{i=1}^n g_i^{(k)}$  and  $\bar{x}^{(k)} := \frac{1}{n} \sum_{i=1}^n x_i^{(k)}$  denote the average gradient and average iterate, respectively. Let  $\Delta_x^{(k)} := \mathbf{x}^{(k)} - E_n \mathbf{x}^{(k)}$  denote the consensus error matrix. For notational convenience, we define

$$C_A := n^{3/2} \eta^{-1} \cdot \frac{1 + \eta}{1 - \eta}, \quad C_W := \frac{n}{1 - \eta}, \quad \beta := \sqrt[3]{1 - \eta},$$

which appear in (5) and (9), respectively. We denote the product of row-stochastic matrices  $\prod_{r=0}^{R_k-1} A^{(k,r)}$  by  $A^{(k)}$ , and write  $W^{(k)}$  for  $W^{(k,R_k)}$ . Finally, when there is no ambiguity, a row vector resulting from vector-matrix multiplication (e.g.,  $\mathbf{1}_n^\top \mathbf{x}^{(k)}$ ) is treated as a column vector when added to or subtracted from other column vectors.

As is standard in the analysis of decentralized gradient descent, the key step is to establish a descent property with respect to the consensus quantities  $\bar{x}^{(k)}$  and  $\bar{g}^{(k)}$ . This is formalized in Lemma 1.

**Lemma 1.** *Suppose Assumptions 1–4 hold for Algorithm 3. When  $\gamma \leq \frac{1}{6L}$  and  $R_k \geq \ln(C_W)/\ln(1/\beta)$ , for any  $k \geq 0$ , we have*

$$\begin{aligned} \frac{\gamma}{4} \|\bar{g}^{(k)}\|^2 + \frac{\gamma}{6} \|\nabla f(\bar{x}^{(k)})\|^2 &\leq (1 + 8\gamma L C_W^2 \beta^{2R_k}) (f(\bar{x}^{(k)}) - f^*) \\ &\quad - (f(\bar{x}^{(k+1)}) - f^*) + \frac{2}{\gamma} \|\Delta_x^{(k)}\|_F^2, \end{aligned} \quad (14)$$

where  $f^* := n^{-1} \sum_{i=1}^n \inf_{x \in \mathbb{R}^d} f_i(x)$ .

*Proof.* See Appendix A.6. □

Beyond the optimality of  $\bar{x}^{(k)}$ , achieving consensus is equally important. To this end, we analyze the evolution of the consensus error matrix  $\Delta_x^{(k)}$  in Lemma 2.

**Lemma 2.** Suppose Assumptions 1–4 hold for Algorithm 3. When  $\gamma \leq \frac{1}{6L}$  and  $R_k \geq \max\{\ln(C_W)/\ln(1/\beta), \ln(3C_A)/\ln(1/\beta)\}$ , we have

$$\|\Delta_x^{(k+1)}\|_F^2 \leq \frac{1}{3}\|\Delta_x^{(k)}\|_F^2 + 8n\gamma^2 LC_W^2 \beta^{2R_k} (f(\bar{x}^{(k)}) - f^*), \quad (15)$$

where  $f^*$  is defined the same as in Lemma 1.

*Proof.* See Appendix A.7. □

Next, multiplying both sides of (15) by  $\frac{12}{\gamma}$  and adding the result to (14) yields

$$\begin{aligned} & \frac{\gamma}{4}\|\bar{g}^{(k)}\|^2 + \frac{\gamma}{6}\|\nabla f(\bar{x}^{(k)})\|^2 + \frac{12}{\gamma}\|\Delta_x^{(k+1)}\|_F^2 \\ & \leq (1 + (8 + 96n)\gamma LC_W^2 \beta^{2R_k})(f(\bar{x}^{(k)}) - f^*) - (f(\bar{x}^{(k+1)}) - f^*) + \frac{6}{\gamma}\|\Delta_x^{(k)}\|_F^2. \end{aligned} \quad (16)$$

Since the coefficients of  $f(\bar{x}^{(k)}) - f^*$  and  $f(\bar{x}^{(k+1)}) - f^*$  differ, we require the following lemma to account for the resulting discrepancy.

**Lemma 3.** Let  $\{S_k\}_{k=0}^{K-1}$ ,  $\{D_k\}_{k=0}^{K-1}$ , and  $\{F_k\}_{k=0}^{K-1}$  be three sequences of positive values, and let  $c > 0$  be a constant. If the inequality

$$S_k \leq \left(1 + \frac{c}{(k+1)^2}\right) D_k - D_{k+1} + F_k \quad (17)$$

holds for all  $0 \leq k \leq K-1$ , then

$$\sum_{k=0}^{K-1} S_k \leq e^{2c} D_0 + \frac{e^{2c}}{1+c} \sum_{k=0}^{K-1} F_k. \quad (18)$$

*Proof.* See Appendix A.8. □

To apply Lemma 3, we require  $(8 + 96n)\gamma LC_W^2 \beta^{2R_k} \leq c/(1+k)^2$ . A sufficient condition is  $\gamma \leq (16 \cdot (1 + 12n)LC_W^2)^{-1}$  and  $R_k \geq \ln(1+k)/\ln(1/\beta)$ . With this choice, we have  $c = \frac{1}{2}$  in (17) and  $e^{2c} < 3$ . Setting  $S_k = \frac{\gamma}{4}\|\bar{g}^{(k)}\|^2 + \frac{\gamma}{6}\|\nabla f(\bar{x}^{(k)})\|^2 + \frac{12}{\gamma}\|\Delta_x^{(k+1)}\|_F^2$ ,  $D_k = f(\bar{x}^{(k)}) - f^*$ ,  $F_k = \frac{6}{\gamma}\|\Delta_x^{(k)}\|_F^2$ , and applying (18), we obtain

$$\begin{aligned} & \frac{\gamma}{4} \sum_{k=0}^{K-1} \|\bar{g}^{(k)}\|^2 + \frac{\gamma}{6} \sum_{k=0}^{K-1} \|\nabla f(\bar{x}^{(k)})\|^2 + \frac{12}{\gamma} \sum_{k=1}^K \|\Delta_x^{(k)}\|_F^2 \\ & \leq 3(f(\bar{x}^{(0)}) - f^*) + \frac{12}{\gamma} \sum_{k=0}^{K-1} \|\Delta_x^{(k)}\|_F^2. \end{aligned} \quad (19)$$

Note that Algorithm 3 is initialized at consensus, so  $\Delta_x^{(0)} = 0$ . Substituting the definitions of  $C_A$ ,  $C_W$ , and  $\beta$  into the above bounds, we obtain our main result:

**Theorem 2 (CONVERGENCE PROPERTY).** Suppose Assumptions 1–4 hold for Algorithm 3. If we choose the step size  $\gamma \leq \frac{(1-\eta)^2}{16n^2(1+12n)L}$ , and the inner iteration rounds

$$\begin{aligned} R_k & \geq \max\{\ln(3C_A)/\ln(1/\beta), \ln(C_W)/\ln(1/\beta), \ln(1+k)/\ln(1/\beta)\} \\ & = \max\left\{B + \frac{B}{-\ln(1-\eta)} \left(\frac{3}{2} \ln n + \ln\left(3 + \frac{3}{\eta}\right)\right), \frac{B \ln(1+k)}{-\ln(1-\eta)}\right\}, \end{aligned}$$

where  $\eta$  and  $B$  are defined in Proposition 1, we have

$$\frac{1}{K} \sum_{k=0}^{K-1} \|\nabla f(\bar{x}^{(k)})\|^2 \leq \frac{18(f(\bar{x}^{(0)}) - f^*)}{\gamma K}, \quad (20)$$

where  $f^* := n^{-1} \sum_{i=1}^n \inf_{x \in \mathbb{R}^d} f_i(x)$ . The total number of communication rounds is

$$\sum_{k=0}^{K-1} R_k \leq \max \left\{ \sum_{k=0}^{K-1} \frac{\ln(k+1)}{\ln(1/\beta)}, \sum_{k=0}^{K-1} \frac{\ln(3C_A)}{\ln(1/\beta)} \right\} \leq \frac{\max\{K \ln(K), K \ln(3C_A)\}}{\ln(1/\beta)}.$$

*Proof.* See Appendix A.9. □

**Remark 2** (CONVERGENCE IN COMMUNICATION ROUNDS). In Theorem 2, we define the total number of communication rounds as  $T = \sum_{k=0}^{K-1} R_k$  and obtain  $K = \mathcal{O}(T/\ln(T))$ . Substituting this into (20) yields:

$$\frac{1}{K} \sum_{k=0}^{K-1} \|\nabla f(\bar{x}^{(k)})\|^2 = \mathcal{O}\left(\frac{\ln(T)}{T}\right). \quad (21)$$

This complexity is nearly the same order as decentralized optimization over doubly-stochastic [48] or column-stochastic mixing matrices [33], except for an additional  $\ln(T)$  factor. To the best of our knowledge, PULM-DGD is the first approach that achieves convergence for decentralized optimization over TVBNs with highly dynamic row-stochastic mixing matrices.

## 5 Experiments

To verify the effectiveness of Algorithms 2 and 3, we conducted extensive experiments across various problem types and time-varying network topologies. We considered three problem settings: (i) average consensus, (ii) logistic regression with non-convex regularization, and (iii) neural network training for MNIST and CIFAR-10 classification. In this section, we present representative experimental results; additional experiments, details on problem settings, and network topology selection strategies can be found in Appendix B.

### 5.1 Comparison with Push-Family Algorithms

PUSH-DIGING [9] and its consensus counterpart PUSH-SUM [29] are among the few methods that explicitly address time-varying directed networks. However, as shown in Section 1.1, push-based schemes require knowledge of out-degrees to construct column-stochastic mixing weights. Under packet loss, the *effective* out-degree becomes random and time-varying: although a node transmits to all out-neighbors, only a subset of messages is successfully received. Since the nominal out-degree does not reflect actual deliveries, the resulting mixing matrix may not be column-stochastic, causing Push-Family to become unstable and potentially fail to converge. In contrast, PULM-Family remains robust (Figure 4).

The first plot of Figure 4 shows average consensus performance with  $N = 20$  nodes and random  $d = 1024$ -dimensional data; the communication graph is resampled at each iteration with sparsity  $s = 0.2$ . The

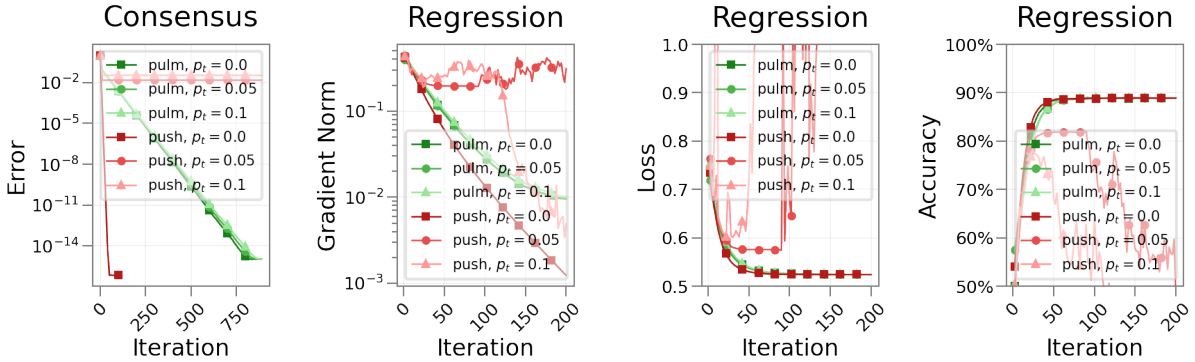


Figure 4: Performance comparison of push-family and PULM-family algorithms under packet loss on time-varying directed networks. In consensus, `push` denotes push-sum and `pulm` denotes PULM; in regression, `push` denotes push-DIGing and `pulm` denotes PULM-DGD. The packet-loss probability is  $p_t$ . See Appendix B for full experimental settings.

remaining panels present regression results on synthetic data: 10 nodes each hold 1000 samples with 30 features, the heterogeneity parameter is  $\sigma_h = 0.1$ , and the stepsize is  $\gamma = 0.1$ . Communication uses a fixed strongly connected graph with sparsity 0.3, where links disconnect with probability  $p_d = 0.4$  (These disconnections are reflected in the out-degrees, which Push-Family algorithms are able to capture. The role of  $p_d$  is to generate time-varying graphs based on a fixed graph). Inner communication rounds are fixed at  $R_k \equiv 10$ . Another more crucial parameter is the packet loss probability  $p_t$  between transmission and reception, which is set as 0.0, 0.05 and 0.1 for both consensus and regression problems. In all cases, push-based methods (push-sum and push-DIGing) are highly sensitive to packet loss—even  $p_t = 0.05$  prevents convergence—whereas PULM and PULM-DGD remain robust, as they do not rely on out-degree information for normalization.

## 5.2 Effect of Different Inner Communication Rounds $R_k$

The inner communication rounds  $R_k$  control the amount of mixing (i.e., consensus refinement) performed per outer iteration and thus directly determine the communication cost. Theorem 2 provides a sufficient choice, requiring  $R_k$  to grow on the order of  $\ln(k)$  to guarantee the stated convergence bound. In practice, however, we observe that constant values of  $R_k$  often yield nearly identical optimization performance, suggesting that the theoretical schedule is conservative.

Figure 5 confirms this empirically: varying  $R_k$  primarily affects communication cost rather than final performance. Across logistic regression, MNIST, and CIFAR-10, the loss and accuracy curves for different  $R_k$  values nearly overlap, indicating that Algorithm 3 is insensitive to this hyperparameter. While larger  $R_k$  can slightly improve early-stage convergence by enhancing mixing, the benefit quickly saturates. Hence, a small constant  $R_k$  is typically sufficient in practice; indeed, even  $R_k = 1$  achieves satisfactory performance across all experiments.

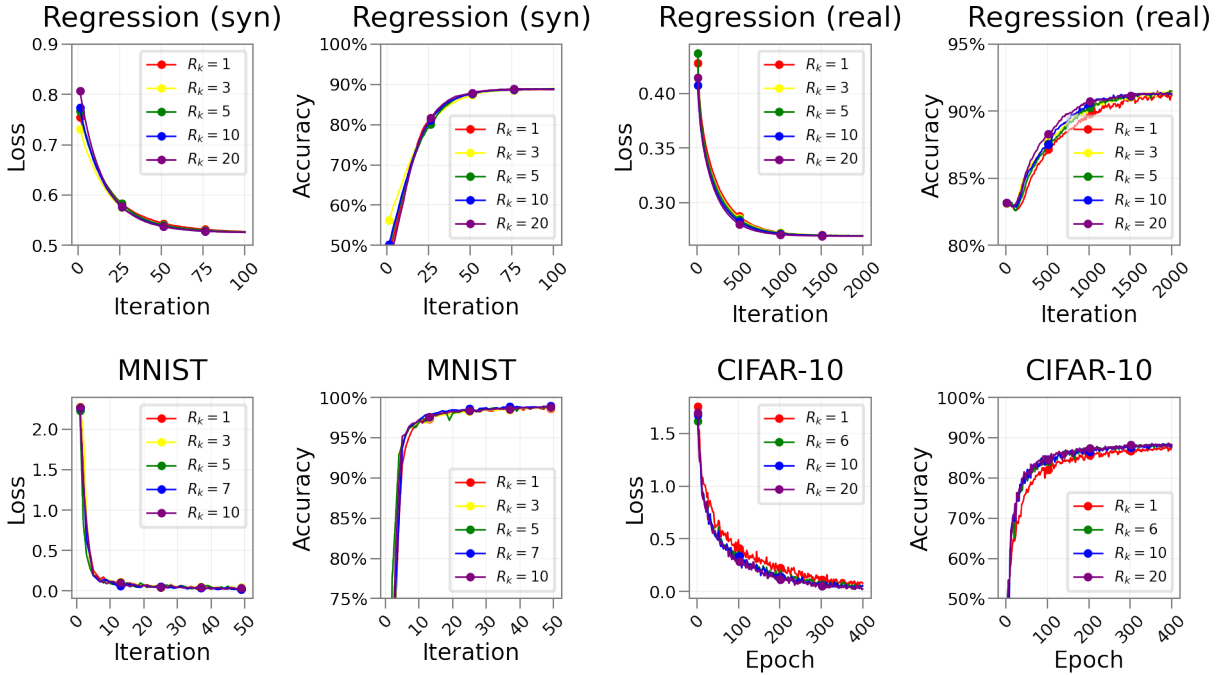


Figure 5: Effect of the inner communication rounds  $R_k$  on the performance of Algorithm 3. Top row: logistic regression on synthetic data (loss and accuracy) and on real data (loss and accuracy) for  $R_k \in \{1, 3, 5, 10, 20\}$ . Bottom row: MNIST training (loss and accuracy) for  $R_k \in \{1, 3, 5, 7, 10\}$ , and CIFAR-10 training (loss and accuracy) for  $R_k \in \{1, 6, 10, 20\}$ . Larger  $R_k$  increases communication per outer iteration but yields only marginal changes in convergence behavior. See Appendix B.5 for experimental details.

## 6 Conclusion

In this paper, we studied decentralized optimization over time-varying broadcast networks (TVBNs). We showed that the limiting Perron vector induced by the mixing process can be future-dependent, rendering existing pre-correction strategies inapplicable. To address this challenge, we proposed PULM, a row-stochastic, broadcast-compatible protocol that achieves average consensus at an exponential rate. We further integrated PULM with distributed gradient descent to obtain PULM-DGD, where model parameters are propagated via standard broadcast while gradients are mixed using PULM. Under standard assumptions for nonconvex objectives, PULM-DGD achieves a convergence rate of  $\mathcal{O}(\ln(T)/T)$  in communication rounds, nearly matching methods using doubly-stochastic or column-stochastic mixing. Future work includes developing single-loop algorithms for decentralized optimization over row-stochastic digraphs.

## References

- [1] R Olfati Saber and Richard M Murray. Agreement problems in networks with directed graphs and switching topology. In *42nd IEEE International Conference on Decision and Control (IEEE Cat. No.*

- 03CH37475), volume 4, pages 4126–4132. IEEE, 2003.
- [2] Ola Shorinwa, Trevor Halsted, Javier Yu, and Mac Schwager. Distributed optimization methods for multi-robot systems: Part 1—a tutorial [tutorial]. *IEEE Robotics & Automation Magazine*, 31(3):121–138, 2024.
- [3] Lifeng Sang, Anish Arora, and Hongwei Zhang. On link asymmetry and one-way estimation in wireless sensor networks. *ACM Transactions on Sensor Networks (TOSN)*, 6(2):1–25, 2010.
- [4] Soumya Kar and José MF Moura. Distributed consensus algorithms in sensor networks with imperfect communication: Link failures and channel noise. *IEEE Transactions on Signal Processing*, 57(1):355–369, 2008.
- [5] Zhen Zhang, Chaokun Chang, Haibin Lin, Yida Wang, Raman Arora, and Xin Jin. Is network the bottleneck of distributed training? In *Proceedings of the Workshop on Network Meets AI & ML*, pages 8–13, 2020.
- [6] Feng Liang, Zhen Zhang, Haifeng Lu, Victor Leung, Yanyi Guo, and Xiping Hu. Communication-efficient large-scale distributed deep learning: A comprehensive survey. *arXiv preprint arXiv:2404.06114*, 2024.
- [7] Angelia Nedić and Alex Olshevsky. Distributed optimization over time-varying directed graphs. *IEEE Transactions on Automatic Control*, 60(3):601–615, 2014.
- [8] Angelia Nedić and Alex Olshevsky. Stochastic gradient-push for strongly convex functions on time-varying directed graphs. *IEEE Transactions on Automatic Control*, 61(12):3936–3947, 2016.
- [9] A. Nedic, A. Olshevsky, and W. Shi. Achieving geometric convergence for distributed optimization over time-varying graphs. *SIAM Journal on Optimization*, 27(4):2597–2633, 2017.
- [10] Fakhteh Saadatniaki, Ran Xin, and Usman A Khan. Decentralized optimization over time-varying directed graphs with row and column-stochastic matrices. *IEEE Transactions on Automatic Control*, 65(11):4769–4780, 2020.
- [11] Angelia Nedić, Duong Thuy Anh Nguyen, and Duong Tung Nguyen. Ab/push-pull method for distributed optimization in time-varying directed networks. *Optimization Methods and Software*, pages 1–28, 2023.
- [12] Duong Thuy Anh Nguyen, Duong Tung Nguyen, and Angelia Nedić. Accelerated ab/push–pull methods for distributed optimization over time-varying directed networks. *IEEE Transactions on Control of Network Systems*, 11(3):1395–1407, 2023.
- [13] Mohammad Akbari, Bahman Ghahesifard, and Tamás Linder. Distributed online convex optimization on time-varying directed graphs. *IEEE Transactions on Control of Network Systems*, 4(3):417–428, 2015.

- [14] Stephen Boyd, Arpita Ghosh, Balaji Prabhakar, and Devavrat Shah. Randomized gossip algorithms. *IEEE transactions on information theory*, 52(6):2508–2530, 2006.
- [15] Tuncer Can Aysal, Mehmet Ercan Yildiz, Anand D Sarwate, and Anna Scaglione. Broadcast gossip algorithms for consensus. *IEEE Transactions on Signal processing*, 57(7):2748–2761, 2009.
- [16] Van Sy Mai and Eyad H Abed. Distributed optimization over weighted directed graphs using row stochastic matrix. In *2016 American Control Conference (ACC)*, pages 7165–7170. IEEE, 2016.
- [17] Angelia Nedic and Asuman Ozdaglar. Distributed subgradient methods for multi-agent optimization. *IEEE Transactions on Automatic Control*, 54(1):48–61, 2009.
- [18] Jianshu Chen and Ali H Sayed. Diffusion adaptation strategies for distributed optimization and learning over networks. *IEEE Transactions on Signal Processing*, 60(8):4289–4305, 2012.
- [19] John C Duchi, Alekh Agarwal, and Martin J Wainwright. Dual averaging for distributed optimization: Convergence analysis and network scaling. *IEEE Transactions on Automatic control*, 57(3):592–606, 2011.
- [20] Kun Yuan, Qing Ling, and Wotao Yin. On the convergence of decentralized gradient descent. *SIAM Journal on Optimization*, 26(3):1835–1854, 2016.
- [21] Wei Shi, Qing Ling, Gang Wu, and Wotao Yin. Extra: An exact first-order algorithm for decentralized consensus optimization. *SIAM Journal on Optimization*, 25(2):944–966, 2015.
- [22] Kun Yuan, Bicheng Ying, Xiaochuan Zhao, and Ali H Sayed. Exact diffusion for distributed optimization and learning—part i: Algorithm development. *IEEE Transactions on Signal Processing*, 67(3):708–723, 2018.
- [23] Zhi Li, Wei Shi, and Ming Yan. A decentralized proximal-gradient method with network independent step-sizes and separated convergence rates. *IEEE Transactions on Signal Processing*, 67(17):4494–4506, 2019.
- [24] Jinming Xu, Shanying Zhu, Yeng Chai Soh, and Lihua Xie. Augmented distributed gradient methods for multi-agent optimization under uncoordinated constant stepsizes. In *IEEE Conference on Decision and Control (CDC)*, pages 2055–2060, Osaka, Japan, 2015.
- [25] P. Di Lorenzo and G. Scutari. Next: In-network nonconvex optimization. *IEEE Transactions on Signal and Information Processing over Networks*, 2(2):120–136, 2016.
- [26] Guannan Qu and Na Li. Harnessing smoothness to accelerate distributed optimization. *IEEE Transactions on Control of Network Systems*, 5(3):1245–1260, 2017.

- [27] Marie Maros and Joakim Jaldén. Panda: A dual linearly converging method for distributed optimization over time-varying undirected graphs. In *2018 IEEE Conference on Decision and Control (CDC)*, pages 6520–6525. IEEE, 2018.
- [28] Konstantinos I Tsianos, Sean Lawlor, and Michael G Rabbat. Push-sum distributed dual averaging for convex optimization. In *2012 IEEE 51st IEEE conference on decision and control (cdc)*, pages 5453–5458. IEEE, 2012.
- [29] David Kempe, Alin Dobra, and Johannes Gehrke. Gossip-based computation of aggregate information. In *44th Annual IEEE Symposium on Foundations of Computer Science, 2003. Proceedings.*, pages 482–491. IEEE, 2003.
- [30] Jinshan Zeng and Wotao Yin. Extrapush for convex smooth decentralized optimization over directed networks. *Journal of Computational Mathematics*, pages 383–396, 2017.
- [31] Chenguang Xi and Usman A Khan. Dextra: A fast algorithm for optimization over directed graphs. *IEEE Transactions on Automatic Control*, 62(10):4980–4993, 2017.
- [32] Chenguang Xi, Ran Xin, and Usman A Khan. Add-opt: Accelerated distributed directed optimization. *IEEE Transactions on Automatic Control*, 63(5):1329–1339, 2017.
- [33] Liyuan Liang, Xinmeng Huang, Ran Xin, and Kun Yuan. Towards better understanding the influence of directed networks on decentralized stochastic optimization. *arXiv preprint arXiv:2312.04928*, 2023.
- [34] Ali H Sayed. Adaptive networks. *Proceedings of the IEEE*, 102(4):460–497, 2014.
- [35] Chenguang Xi, Van Sy Mai, Ran Xin, Eyad H Abed, and Usman A Khan. Linear convergence in optimization over directed graphs with row-stochastic matrices. *IEEE Transactions on Automatic Control*, 63(10):3558–3565, 2018.
- [36] Huaqing Li, Jinneng Wang, and Zheng Wang. Row-stochastic matrices based distributed optimization algorithm with uncoordinated step-sizes. In *2019 6th International Conference on Information, Cybernetics, and Computational Social Systems (ICCSS)*, pages 124–131. IEEE, 2019.
- [37] Ran Xin, Chenguang xi, and Usman Khan. Frost—fast row-stochastic optimization with uncoordinated step-sizes. *EURASIP Journal on Advances in Signal Processing*, 2019, 01 2019.
- [38] Liyuan Liang, Xinyi Chen, Gan Luo, and Kun Yuan. Achieving linear speedup and near-optimal complexity for decentralized optimization over row-stochastic networks. In *Forty-second International Conference on Machine Learning*, 2025.
- [39] Diyako Ghaderyan, Necdet Serhat Aybat, A Pedro Aguiar, and Fernando Lobo Pereira. A fast row-stochastic decentralized method for distributed optimization over directed graphs. *IEEE Transactions on Automatic Control*, 69(1):275–289, 2023.

- [40] Qingguo Lü, Xiaofeng Liao, Huaqing Li, and Tingwen Huang. A nesterov-like gradient tracking algorithm for distributed optimization over directed networks. *IEEE Transactions on Systems, Man, and Cybernetics: Systems*, 51(10):6258–6270, 2020.
- [41] Shi Pu, Wei Shi, Jinming Xu, and Angelia Nedić. Push–pull gradient methods for distributed optimization in networks. *IEEE Transactions on Automatic Control*, 66(1):1–16, 2020.
- [42] Ran Xin and Usman A Khan. A linear algorithm for optimization over directed graphs with geometric convergence. *IEEE Control Systems Letters*, 2(3):315–320, 2018.
- [43] Runze You and Shi Pu. Stochastic push-pull for decentralized nonconvex optimization. *arXiv preprint arXiv:2506.07021*, 2025.
- [44] Liyuan Liang, Gan Luo, and Kun Yuan. On the linear speedup of the push-pull method for decentralized optimization over digraphs. *arXiv preprint arXiv:2506.18075*, 2025.
- [45] Angelia Nedić, Duong Thuy Anh Nguyen, and Duong Tung Nguyen. Ab/push-pull method for distributed optimization in time-varying directed networks. *Optimization Methods and Software*, 40(5):1044–1071, 2025.
- [46] Orhan Eren Akgün, Arif Kerem Dayı, Stephanie Gil, and Angelia Nedić. Projected push-pull for distributed constrained optimization over time-varying directed graphs. In *2024 American Control Conference (ACC)*, pages 2082–2089. IEEE, 2024.
- [47] Brendan McMahan, Eider Moore, Daniel Ramage, Seth Hampson, and Blaise Aguera y Arcas. Communication-Efficient Learning of Deep Networks from Decentralized Data. In Aarti Singh and Jerry Zhu, editors, *Proceedings of the 20th International Conference on Artificial Intelligence and Statistics*, volume 54 of *Proceedings of Machine Learning Research*, pages 1273–1282. PMLR, 20–22 Apr 2017.
- [48] Sulaiman A Alghunaim and Kun Yuan. A unified and refined convergence analysis for non-convex decentralized learning. *IEEE Transactions on Signal Processing*, 70:3264–3279, 2022.
- [49] Angelia Nedić and Asuman Ozdaglar. Convergence rate for consensus with delays. *Journal of Global Optimization*, 47(3):437–456, July 2010.

## A Proof Details and Supplementary Lemmata

### A.1 Proof of Proposition 1

*Proof.* We introduce the following notation: (i)  $v_1 \rightarrow v_2$  indicates that there exists an edge from  $v_1$  to  $v_2$  in a given graph  $\mathcal{G}$  (where  $\mathcal{G}$  may be an accumulated graph as defined in Assumption 1); (ii)  $v_1 \xrightarrow{t} v_2$  indicates that  $v_1$  sends information to  $v_2$  at time  $t$ , i.e.,  $(v_1, v_2) \in \mathcal{E}^{(t)}$ .

It suffices to show that for any starting time  $k$ , any source node  $s \in \mathcal{V}$ , and any destination node  $e \in \mathcal{V}$ , there exists a finite-length path from  $s$  to  $e$  whose length is independent of  $k$ . By Assumption 1, self-loops exist at every node. Let  $B$  denote the maximum path length among all source-destination pairs, and extend each shorter path to length  $B$  by appending self-loops. Applying the Chapman–Kolmogorov equation, we obtain

$$\left[ \prod_{l=k}^{k+B-1} A^{(l)} \right]_{e,s} \geq [A^{(k+B-1)}]_{e,v_{B-1}} \cdots [A^{(k+1)}]_{v_2,v_1} [A^{(k)}]_{v_1,s} \geq \tau^B,$$

where  $s \xrightarrow{k} v_1 \xrightarrow{k+1} v_2 \cdots \xrightarrow{k+B-2} v_{B-1} \xrightarrow{k+B-1} e$  is a given state transition trajectory with length  $B$ , and the second inequality is from Assumption 3.

Since directed graphs always contain self-loops, the case  $s = e$  is trivial. For  $s \neq e$ , we define  $\mathcal{V}_\ominus$  as the set of nodes that have already been visited, initialized as  $\mathcal{V}_\ominus = \{s\}$ , and expand this set during the search process. The searching process can be broken down into the following steps.

**Step 1.** Use Assumption 1, during  $\tilde{B}$  time intervals, we can find at least one path from  $s$  to  $e$ , from which we pick out a shortest path  $s \rightarrow v_1 \rightarrow \cdots \rightarrow e$ . We add  $v_1$  into  $\mathcal{V}_\ominus$ , and there exists at least one time point  $t_1 \in [k, k + \tilde{B} - 1]$  such that  $(s, v_1) \in \mathcal{E}^{(t_1)}$ . We construct the trajectory as

$$s \xrightarrow{k} s \xrightarrow{k+1} \cdots s \xrightarrow{t_1-1} s \xrightarrow{t_1} v_1,$$

and record the time point  $t_1$ . Then go to Step 2.

**Step 2.** Rename the latest added node as  $v_-$  and the latest recorded time point as  $t_-$ . If  $v_- = e$ , go to Step 4. Otherwise, go to Step 3.

**Step 3.** Changing starting node as  $v_-$  and time point as  $t_- + 1$ , using Assumption 1 again, during  $\tilde{B}$  time intervals, we can find at least one path from  $v_-$  to  $e$ , from which we pick out a shortest path  $v_- \rightarrow \cdots \rightarrow v_\times \rightarrow v_+ \rightarrow \cdots \rightarrow e$ , where  $v_\times$  is the last node which still stays in  $\mathcal{V}_\ominus$  and  $v_+$  is the first node not in  $\mathcal{V}_\ominus$ . We denote the first time point when  $v_\times$  is searched as  $t_\times$ . Then there exists at least one time point  $t_+ \in [t_\times + 1, t_\times + \tilde{B}]$  such that  $(v_\times, v_+) \in \mathcal{E}^{(t_+)}$ . We continue the trajectory from time point  $t_\times$  as

$$\cdots \xrightarrow{t_\times} v_\times \xrightarrow{t_\times+1} \cdots v_\times \xrightarrow{t_+-1} v_\times \xrightarrow{t_+} v_+.$$

It should be noticed that if  $v_\times \neq v_-$ , we have  $t_\times < t_-$ . In this case, the state transition trajectory is partially reconstructed. After adding  $v_+$  into  $\mathcal{V}_\ominus$  and recording the new time point  $t_+$ , we go back to Step 2.

**Step 4.** The searching process is finished, and a state transition trajectory has been constructed.

As the set of searched nodes  $\mathcal{V}_\ominus$  expands continuously, Step 3 will be repeated no more than  $n - 1$  times. We can find a state transition trajectory starting at time point  $k$  from  $s$  to  $e$  whose length  $B$  is no longer than  $n\tilde{B}$ . Together with the claim at the beginning of the proof, the existence of  $B$  and  $\eta$  is proved.  $\square$

## A.2 Linear Convergence Lemma for Positive Mixing Matrices

**Lemma 4.** For a sequence of row-stochastic matrices  $\tilde{A}^{(1)}, \tilde{A}^{(2)}, \dots \in \mathbb{R}^{n \times n}$ , assuming  $\tilde{A}_{i,j}^{(t)} \geq \eta > 0$ ,  $\forall i, j \in [n]$ ,  $\forall t = 1, 2, \dots$ , we have

(i) The limit  $\tilde{A}^\infty := \prod_{t=1}^{+\infty} \tilde{A}^{(t)}$  exists. And  $\tilde{A}^\infty$  is a row-stochastic matrix with identical rows, i.e.,

$$\tilde{A}^\infty = \mathbf{1}_n \pi^\top,$$

where  $\pi$  is an asymptotical steady distribution determined by the whole sequence  $\{\tilde{A}^{(t)}\}_{t=1}^\infty$ .

(ii) The maximum deviation converges with geometric rate, i.e.,

$$\max \left| \prod_{t=1}^T \tilde{A}^{(t)} - \tilde{A}^\infty \right| \leq \frac{1+\eta}{\eta} (1-\eta)^T$$

*Proof.* The proof technique here is adapted from [17, 49]. However, our lemma is more readily applicable under the milder Assumptions 1, 2, and 3, which were not considered in [17, 49].

**Proof of (i).** Consider an arbitrary vector  $\mathbf{x}^{(0)} \in \mathbb{R}^n$ , we suppose to prove that the limit of  $\mathbf{x}^{(t)} := \tilde{A}^{(t)} \dots \tilde{A}^{(1)} \mathbf{x}^{(0)}$  exists. Note that  $\mathbf{x}^{(t)}$  can be decomposed into a consensus part and a surplus part, i.e.,

$$\mathbf{x}^{(t)} = p^{(t)} \mathbf{1}_n + \mathbf{z}^{(t)}, \quad \mathbf{z}^{(t)} \geq 0. \quad (22)$$

where  $p^{(t)}$  is a scalar and  $\mathbf{z}^{(t)}$  is a vector. Our goal is to construct a Cauchy sequence  $\{p^{(t)}\}_{t=0}^\infty$  and  $\{\mathbf{z}^{(t)}\}_{t=0}^\infty \rightarrow \mathbf{0}$ . We first choose

$$p^{(0)} = \min_{1 \leq i \leq n} \{\mathbf{x}_i^{(0)}\}, \quad \mathbf{z}^{(0)} = \mathbf{x}^{(0)} - \min_{1 \leq i \leq n} \{\mathbf{x}_i^{(0)}\} \mathbf{1}_n.$$

Using the decomposition, the recursion of  $\mathbf{x}^{(t)}$  can be expanded as

$$\mathbf{x}^{(t+1)} = \tilde{A}^{(t+1)} \mathbf{x}^{(t)} = \tilde{A}^{(t+1)} (p^{(t)} \mathbf{1}_n + \mathbf{z}^{(t)}) = p^{(t)} \mathbf{1}_n + \tilde{A}^{(t+1)} \mathbf{z}^{(t)}.$$

We define the index  $i^*$  as

$$i^* := \arg \min_{1 \leq i \leq n} \tilde{A}_{i,\cdot}^{(t+1)} \mathbf{z}^{(t)},$$

which means  $\min_{1 \leq i \leq n} \{\tilde{A}_{i,\cdot}^{(t+1)} \mathbf{z}^{(t)}\} = \tilde{A}_{i^*,\cdot}^{(t+1)} \mathbf{z}^{(t)}$ . And we further specify  $\mathbf{z}^{(t+1)}$  and  $p^{(t+1)}$  as

$$\mathbf{z}^{(t+1)} = \tilde{A}^{(t+1)} \mathbf{z}^{(t)} - (\tilde{A}_{i^*,\cdot}^{(t+1)} \mathbf{z}^{(t)}) \mathbf{1}_n, \quad p^{(t+1)} = p^{(t)} + \tilde{A}_{i^*,\cdot}^{(t+1)} \mathbf{z}^{(t)}.$$

Because matrices  $\tilde{A}^{(t)}$  are row-stochastic, according to our choice of  $p^{(t)}$  and  $\mathbf{z}^{(t)}$ , all  $\mathbf{z}^{(t)}$  are non-negative with minimum zero.

Next we prove the geometric convergence of  $\mathbf{z}^{(t)}$ . Consider each entry of  $\mathbf{z}^{(t+1)}$ , for  $i = 1, \dots, n$ ,

$$z_i^{(t+1)} = \tilde{A}_{i,\cdot}^{(t+1)} \mathbf{z}^{(t)} - \tilde{A}_{i^*,\cdot}^{(t+1)} \mathbf{z}^{(t)}.$$

We divide the indices  $i = 1, \dots, n$  into two subsets of  $\{1, \dots, n\}$ :

$$J^+ := \{j | \tilde{A}_{i,j}^{(t+1)} - \tilde{A}_{i^*,j}^{(t+1)} \geq 0\}, \quad J^- := \{j | \tilde{A}_{i,j}^{(t+1)} - \tilde{A}_{i^*,j}^{(t+1)} < 0\}.$$

Since  $\tilde{A}^{(t+1)}$  is row-stochastic, the positive index subset  $J^+$  is non-empty. Then, for any  $i \in [n]$ , we have

$$\begin{aligned} 0 \leq \mathbf{z}_i^{(t+1)} &= \tilde{A}_{i,\cdot}^{(t+1)} \mathbf{z}^{(t)} - \tilde{A}_{i^*,\cdot}^{(t+1)} \mathbf{z}^{(t)} = \sum_{1 \leq j \leq n} (\tilde{A}_{i,j}^{(t+1)} - \tilde{A}_{i^*,j}^{(t+1)}) \mathbf{z}_j^{(t)} \\ &\leq \sum_{J^+} (\tilde{A}_{i,j}^{(t+1)} - \tilde{A}_{i^*,j}^{(t+1)}) \mathbf{z}_j^{(t)} \leq \|\mathbf{z}^{(t)}\|_\infty \sum_{J^+} (\tilde{A}_{i,j}^{(t+1)} - \tilde{A}_{i^*,j}^{(t+1)}) \\ &= \|\mathbf{z}^{(t)}\|_\infty \left( \sum_{J^+} \tilde{A}_{i,j}^{(t+1)} - \sum_{J^+} \tilde{A}_{i^*,j}^{(t+1)} \right) \leq (1 - \eta) \|\mathbf{z}^{(t)}\|_\infty, \end{aligned}$$

where the last inequality is because  $\eta \leq \tilde{A}_{i,j}^{(t+1)} \leq 1$ ,  $\forall i, j \in [n]$  and  $\sum_{j=1}^n \tilde{A}_{i,j}^{(t+1)} = 1$ . Then we have

$$\|\mathbf{z}^{(t+1)}\|_\infty \leq (1 - \eta) \|\mathbf{z}^{(t)}\|_\infty, \quad \forall t = 0, 1, \dots,$$

and further

$$\|\mathbf{z}^{(T)}\|_\infty \leq (1 - \eta)^T \|\mathbf{z}^{(0)}\|_\infty.$$

Therefore,  $\mathbf{z}^{(t)} \rightarrow 0$  with geometric rate. On the other hand,

$$\begin{aligned} 0 \leq p^{(t+1)} - p^{(t)} &= \tilde{A}_{i^*,\cdot}^{(t+1)} \mathbf{z}^{(t)} = \sum_{j=1}^n \tilde{A}_{i^*,j}^{(t+1)} \mathbf{z}_j^{(t)} \leq \|\mathbf{z}^{(t)}\|_\infty \sum_{j=1}^n \tilde{A}_{i^*,j}^{(t+1)} \\ &\leq \|\mathbf{z}^{(t)}\|_\infty \leq (1 - \eta)^t \|\mathbf{z}^{(0)}\|_\infty, \end{aligned} \tag{23}$$

implying

$$\begin{aligned} p^{(t)} &= p^{(t)} - p^{(t-1)} + p^{(t-1)} - p^{(t-2)} + \dots + p^{(1)} - p^{(0)} + p^{(0)} \\ &\leq \sum_{i=0}^{t-1} (1 - \eta)^i \|\mathbf{z}^{(0)}\|_\infty + p^{(0)} = \frac{1 - (1 - \eta)^t}{\eta} \|\mathbf{z}^{(0)}\|_\infty + p^{(0)} \leq \frac{1}{\eta} \|\mathbf{z}^{(0)}\|_\infty + p^{(0)}. \end{aligned}$$

Hence, the sequence  $p^{(t)}$  is monotonically increasing and bounded, which implies an existent limit  $\tilde{p}$ .

For any arbitrary  $\mathbf{x}^{(0)} \in \mathbb{R}^n$ , we have  $\mathbf{z}^{(t)} \rightarrow 0$  and  $p^{(t)} \rightarrow \tilde{p}$  (the limit  $\tilde{p}$  is related to  $\mathbf{x}^{(0)}$  and the property of each row-stochastic matrix  $\tilde{A}^{(t)}$ ), which ensures the existence of limit  $\prod_{t=1}^{+\infty} \tilde{A}^{(t)}$ . Specifically, we choose the arbitrary vector  $\mathbf{x}^{(0)}$  as  $n$  unit vectors  $\mathbf{e}_1, \dots, \mathbf{e}_n$ , we can derive,

$$\prod_{t=1}^{+\infty} \tilde{A}^{(t)} = \lim_{t \rightarrow +\infty} \tilde{A}^{(t)} \dots \tilde{A}^{(1)} (\mathbf{e}_1, \dots, \mathbf{e}_n) = (\tilde{p}_1 \mathbf{1}_n, \dots, \tilde{p}_n \mathbf{1}_n),$$

where the exact values of  $\tilde{p}_1, \dots, \tilde{p}_n$  cannot be further determined.

Since each matrix  $\tilde{A}^{(t)}$  is row-stochastic, the finite product  $\prod_{t=1}^T \tilde{A}^{(t)}$  is also row-stochastic, and the limit  $\tilde{A}^\infty = \prod_{t=1}^{+\infty} \tilde{A}^{(t)}$  is still row-stochastic with identical rows. We denote  $\pi := (\tilde{p}_1, \dots, \tilde{p}_n)^\top$ , and then

$$\tilde{A}^\infty = \mathbf{1}_n \pi^\top.$$

Since  $\tilde{p}_1, \dots, \tilde{p}_n$  are determined by the whole matrix sequence and the exact values are implicit, the stacked limit vector  $\pi$  also maintain those properties.

**Proof of (ii).** Still considering an arbitrary  $\mathbf{x}^{(0)} \in \mathbb{R}^n$  with decomposition 22, we have

$$(\tilde{A}^{(t)} \dots \tilde{A}^{(1)})\mathbf{x}^{(0)} - \tilde{A}^\infty \mathbf{x}^{(0)} = \mathbf{x}^{(t)} - \tilde{p}\mathbf{1}_n = \mathbf{z}^{(t)} + (p^{(t)} - \tilde{p})\mathbf{1}_n. \quad (24)$$

The coefficient of the second term can be bounded as

$$0 \leq \tilde{p} - p^{(t)} = \lim_{T \rightarrow +\infty} p^{(T)} - p^{(t)} \leq \lim_{T \rightarrow +\infty} \sum_{s=t}^{T-1} (1-\eta)^s \|\mathbf{z}^{(0)}\|_\infty = \frac{(1-\eta)^t}{\eta} \|\mathbf{z}^{(0)}\|_\infty,$$

where the second inequality is from 23. So the infinite norm of 24 can be bounded as

$$\begin{aligned} & \|(\tilde{A}^{(t)} \dots \tilde{A}^{(1)})\mathbf{x}^{(0)} - \tilde{A}^\infty \mathbf{x}^{(0)}\|_\infty \leq \|\mathbf{z}^{(t)}\|_\infty + (\tilde{p} - p^{(t)}) \\ & \leq (1-\eta)^t \|\mathbf{z}^{(0)}\|_\infty + \frac{(1-\eta)^t}{\eta} \|\mathbf{z}^{(0)}\|_\infty = \frac{1+\eta}{\eta} (1-\eta)^t \|\mathbf{z}^{(0)}\|_\infty. \end{aligned}$$

Substitute  $\mathbf{x}^{(0)}$  with unit vectors  $\mathbf{e}_j$ ,  $j = 1, 2, \dots, n$ , and notice that  $\|\mathbf{z}^{(0)}\|_\infty = \max_{i \in [n]} \mathbf{x}_i^{(0)} - \min_{i \in [n]} \mathbf{x}_i^{(0)} = 1$  for unit vectors  $\mathbf{e}_j$ , we have

$$\|(\tilde{A}^{(t)} \dots \tilde{A}^{(1)})_{\cdot, j} - \tilde{p}_j \mathbf{1}_n\|_\infty \leq \frac{1+\eta}{\eta} (1-\eta)^t.$$

Taking all the columns of  $\prod_{t=1}^T \tilde{A}^{(t)}$ , we obtain the conclusion.  $\square$

### A.3 Proof of Proposition 2

The proof pipeline is using the linear convergence result of Lemma 4 in Appendix A.2, which focuses on positive mixing matrices, and then bounding the remaining factors.

*Proof.* According to Proposition 1, there exists a positive period integer  $B$ . Based on the original sequence  $\{\prod_{i=0}^{k-1} A^{(i)}\}_{k=1}^\infty$ , by adding brackets to every  $B$  factors, we get a new sequence:

$$\tilde{A}^{(t)} \dots \tilde{A}^{(1)} := \left( \prod_{i=(t-1)B}^{tB-1} A^{(i)} \right) \dots \left( \prod_{i=0}^{B-1} A^{(i)} \right), \quad t = 1, 2, \dots,$$

where all the  $\tilde{A}^{(t)}$ ,  $t = 1, 2, \dots$  satisfy  $\tilde{A}_{i,j}^{(t)} \geq \eta > 0$ ,  $\forall i, j \in [n]$ . According to Lemma 4, there exists a limit  $\tilde{A}^\infty := \lim_{t \rightarrow \infty} \tilde{A}^{(t)} \dots \tilde{A}^{(1)} = \mathbf{1}_n \pi^\top$ , and the limit vector  $\pi$  is determined by the whole sequence  $\{\tilde{A}^{(t)}\}_{t=1}^\infty$ .

We next prove the original sequence  $\{\prod_{i=0}^{k-1} A^{(i)}\}_{k=1}^\infty$  converges to the same limit  $\tilde{A}^\infty$ . For a given  $k > 0$ , we make the following decomposition,

$$\begin{aligned} \prod_{i=0}^{k-1} A^{(i)} &= \left( \prod_{i=TB}^{k-1} A^{(i)} \right) \left( \prod_{i=(T-1)B}^{TB-1} A^{(i)} \right) \dots \left( \prod_{i=0}^{B-1} A^{(i)} \right) \\ &:= \tilde{A}^{(-1)} \tilde{A}^{(T)} \dots \tilde{A}^{(1)}, \end{aligned} \quad (25)$$

where  $T = \lfloor k/B \rfloor$ . Using the linear convergence result from Lemma 4, we have:

$$\max \left\| \prod_{t=1}^T \tilde{A}^{(t)} - \tilde{A}^\infty \right\| \leq \frac{1+\eta}{\eta} (1-\eta)^T.$$

Therefore, the total deviation can be bounded as

$$\begin{aligned} \left\| \prod_{i=0}^{k-1} A^{(i)} - \tilde{A}^\infty \right\|_F &= \left\| \tilde{A}^{(-1)} \prod_{t=1}^T \tilde{A}^{(t)} - \tilde{A}^\infty \right\|_F = \left\| \tilde{A}^{(-1)} \left( \prod_{t=1}^T \tilde{A}^{(t)} - \tilde{A}^\infty \right) \right\|_F \\ &\leq \left\| \tilde{A}^{(-1)} \right\|_2 \left\| \prod_{t=1}^T \tilde{A}^{(t)} - \tilde{A}^\infty \right\|_F \leq \sqrt{n} \cdot n \max \left\| \prod_{t=1}^T \tilde{A}^{(t)} - \tilde{A}^\infty \right\| \\ &\leq n^{3/2} \frac{1+\eta}{\eta} (1-\eta)^T, \end{aligned}$$

Without loss of generality, we let  $k > B$ , so that  $T = \lfloor k/B \rfloor \geq k/B - 1$ . The norm can be bounded as

$$\left\| \prod_{i=0}^{k-1} A^{(i)} - \tilde{A}^\infty \right\|_F \leq n^{3/2} \frac{1+\eta}{\eta(1-\eta)} \cdot (\sqrt[B]{1-\eta})^k.$$

Therefore, the limit  $\prod_{i=0}^\infty A^{(i)} = \mathbb{1}_n \pi^\top$  exists and the value is given by the infinite product of  $\{\tilde{A}^{(t)}\}_{t=1}^\infty$ . Further, the convergence is exponentially fast.  $\square$

## A.4 Sub-matrices Inequality

**Lemma 5.** For any  $S$  row-stochastic matrices  $A^{(1)}, \dots, A^{(S)} \in \mathbb{R}^{n \times n}$ , we have

$$0 \leq \prod_{s=1}^S A_{-\ell, -\ell}^{(s)} \leq \left( \prod_{s=1}^S A^{(s)} \right)_{-\ell, -\ell},$$

where  $M_{-\ell, -\ell}$  represents the  $(n-1) \times (n-1)$  matrix obtained by removing the  $\ell$ -th row and the  $\ell$ -th column of  $M \in \mathbb{R}^{n \times n}$ .

*Proof.* The left inequality is trivial as non-negative combination cannot produce negative elements. For the right inequality, it is sufficient only to consider the case  $S = 2$ . The case  $S > 2$  can be obtained by mathematical induction. Without loss of generality, we let  $\ell = 1$  to simplify our notation. In this way,

$$A^{(1)} A^{(2)} = \begin{bmatrix} A_{1,1}^{(1)} & A_{1,-1}^{(1)} \\ A_{-1,1}^{(1)} & A_{-1,-1}^{(1)} \end{bmatrix} \begin{bmatrix} A_{1,1}^{(2)} & A_{1,-1}^{(2)} \\ A_{-1,1}^{(2)} & A_{-1,-1}^{(2)} \end{bmatrix}.$$

Hence,

$$(A^{(1)} A^{(2)})_{-1, -1} = A_{-1,1}^{(1)} A_{1,-1}^{(2)} + A_{-1,-1}^{(1)} A_{-1,-1}^{(2)},$$

where  $A_{-1,1}^{(1)} A_{1,-1}^{(2)}$  is a 1-rank matrix generated by two vectors. Since all entries of  $A_{-1,1}^{(1)}$  and  $A_{1,-1}^{(2)}$  are non-negative, we have  $A_{-1,1}^{(1)} A_{1,-1}^{(2)} \geq 0$ , which leads to the conclusion.  $\square$

## A.5 Proof of Theorem 1

*Proof.* We first establish the monotonicity of  $W^{(k)}$ , and then prove its exponential convergence rate. The convergence of  $\mathbf{z}^{(k)}$  follows as a direct corollary.

**Proof of (i).** Let  $X_{i,j}$  denote the  $(i,j)$ -th entry of  $X \in \mathbb{R}^{n \times n}$ , and let  $X_{-i,-j}$  denote the  $(n-1) \times (n-1)$  submatrix obtained by removing the  $i$ -th row and  $j$ -th column of  $X$ . The notations  $X_{i,-j}$  and  $X_{-i,j}$  are defined similarly.

Now we consider the  $\ell$ -th column of  $W^{(k)}$  generated by Algorithm 1, which we denote as  $W_{\cdot,\ell}^{(k)}$ . According to the algorithm,  $W_{\ell,\ell}^{(k)} = 1/n$ . When  $i \neq \ell$ , we have

$$W_{i,\ell}^{(k+1)} - 1/n = \sum_{j=1}^n A_{i,j}^{(k)} W_{j,\ell}^{(k)} - \frac{1}{n} = \sum_{j=1, j \neq \ell}^n A_{i,j}^{(k)} (W_{j,\ell}^{(k)} - 1/n).$$

The last equation utilizes the fact that the row sum of  $A^{(k)} = 1$  and  $W_{\ell,\ell}^{(k)} = 1/n$ . Consider each row of  $W_{\cdot,\ell}^{(k)}$  except the  $\ell$ -th row:

$$\begin{aligned} W_{-\ell,\ell}^{(k+1)} - n^{-1} \mathbf{1}_{n-1} &= \underbrace{[W_{1,\ell}^{(k+1)} - n^{-1}, \dots, W_{n,\ell}^{(k+1)} - n^{-1}]^\top}_{\text{without } \ell\text{-th row}} \\ &= \left[ \underbrace{\sum_{j \neq \ell} A_{1,j}^{(k)} (W_{j,\ell}^{(k)} - 1/n), \dots, \sum_{j \neq \ell} A_{n,j}^{(k)} (W_{j,\ell}^{(k)} - 1/n)}_{\text{without } \ell\text{-th row}} \right]^\top \\ &= A_{-\ell,-\ell}^{(k)} (W_{-\ell,\ell}^{(k)} - n^{-1} \mathbf{1}_{n-1}) \end{aligned} \quad (26)$$

Take the infinite norm on both sides of the equation and use the inequality between the vector norm and the corresponding matrix norm, we have

$$\begin{aligned} \|W_{-\ell,\ell}^{(k+1)} - n^{-1} \mathbf{1}_{n-1}\|_\infty &= \|A_{-\ell,-\ell}^{(k)} (W_{-\ell,\ell}^{(k)} - n^{-1} \mathbf{1}_{n-1})\|_\infty \\ &\leq \|A_{-\ell,-\ell}^{(k)}\|_\infty \|W_{-\ell,\ell}^{(k)} - n^{-1} \mathbf{1}_{n-1}\|_\infty \end{aligned}$$

On one hand, we have  $\|A_{-\ell,-\ell}^{(k)}\|_\infty \leq 1$ , since  $A^{(k)}$  is non-negative and the row sum of  $A^{(k)}$  is no more than 1. On the other hand,

$$\|W_{-\ell,\ell}^{(k)} - n^{-1} \mathbf{1}_{n-1}\|_\infty = \max |W_{-\ell,\ell}^{(k)} - n^{-1} \mathbf{1}_{n-1}| = \max |W_{\cdot,\ell}^{(k)} - n^{-1} \mathbf{1}_n|.$$

Therefore, for each column of  $W^{(k)}$ , we have

$$\max |W_{\cdot,\ell}^{(k+1)} - n^{-1} \mathbf{1}_n| \leq \max |W_{\cdot,\ell}^{(k)} - n^{-1} \mathbf{1}_n|.$$

Taking all columns of  $W^{(k)}$  into consideration, we have

$$\max |W^{(k+1)} - E_n| \leq \max |W^{(k)} - E_n|,$$

which indicates that the sequence  $\{\max |W^{(k)} - n^{-1} \mathbf{1}_n \mathbf{1}_n^\top|\}_{k \geq 0}$  is non-increasing.

**Proof of (ii).** Using (26) recurrently and noticing  $W_{-\ell,\ell}^{(0)} = \mathbf{0}_{n-1}$ , we have

$$W_{-\ell,\ell}^{(k)} - n^{-1}\mathbf{1}_{n-1} = \left( \prod_{i=0}^{k-1} A_{-\ell,-\ell}^{(i)} \right) (-n^{-1}\mathbf{1}_{n-1}),$$

implying

$$\begin{aligned} \|W_{-\ell,\ell}^{(k)} - n^{-1}\mathbf{1}_{n-1}\|_2 &\leq \left\| \prod_{i=0}^{k-1} A_{-\ell,-\ell}^{(i)} \right\|_2 \cdot \|n^{-1}\mathbf{1}_{n-1}\|_2 \\ &\leq \frac{1}{\sqrt{n}} \left\| \prod_{i=0}^{k-1} A_{-\ell,-\ell}^{(i)} \right\|_2 \leq \frac{1}{\sqrt{n}} \left\| \prod_{i=0}^{k-1} A_{-\ell,-\ell}^{(i)} \right\|_F. \end{aligned} \quad (27)$$

Considering the product of  $k$  row-stochastic sub-matrices, under the conclusion of Proposition 1, we suppose  $k > B$ . Denoting  $T = \lfloor k/B \rfloor$ , we use the similar decomposition as (25) and then

$$\begin{aligned} \prod_{i=0}^{k-1} A_{-\ell,-\ell}^{(i)} &= \left( \prod_{i=TB}^{k-1} A_{-\ell,-\ell}^{(i)} \right) \left( \prod_{i=(T-1)B}^{TB-1} A_{-\ell,-\ell}^{(i)} \right) \cdots \left( \prod_{i=0}^{B-1} A_{-\ell,-\ell}^{(i)} \right) \\ &\leq \left( \prod_{i=TB}^{k-1} A^{(i)} \right)_{-\ell,-\ell} \left( \prod_{i=(T-1)B}^{TB-1} A^{(i)} \right)_{-\ell,-\ell} \cdots \left( \prod_{i=0}^{B-1} A^{(i)} \right)_{-\ell,-\ell} \\ &= \tilde{A}_{-\ell,-\ell}^{(-1)} \tilde{A}_{-\ell,-\ell}^T \cdots \tilde{A}_{-\ell,-\ell}^1, \end{aligned}$$

where the inequality is due to Lemma 5 introduced in Appendix A.4 and  $\tilde{A}_{-\ell,-\ell}^{(t)}$  is defined in (25). From Proposition 1 we know that  $\tilde{A}_{i,j}^{(t)} \geq \eta, \forall i, j \in [n]$ , so each row sum of  $\tilde{A}_{-\ell,-\ell}^{(t)}$  is no more than  $1 - \eta$ . Next, we can prove that for two series of non-negative scalars  $a_1, \dots, a_{n-1}; b_1, \dots, b_{n-1}$ , if  $\sum_{i=1}^{n-1} a_i \leq 1 - \eta$ , then  $\sum_{i=1}^{n-1} a_i b_i \leq (1 - \eta) \max_i \{b_i\}$ . Now consider two non-negative matrices  $A, B \in \mathbb{R}^{(n-1) \times (n-1)}$ , if each row sum of  $A$  is no more than  $1 - \eta$ , we have  $(AB)_{i,j} = \sum_{k=1}^{n-1} A_{i,k} B_{k,j} \leq (1 - \eta) \max_k B_{k,j}$ . By choosing  $A = \tilde{A}_{-\ell,-\ell}^{(t+1)}$ ,  $B = \tilde{A}_{-\ell,-\ell}^{(t)} \cdots \tilde{A}_{-\ell,-\ell}^{(1)}$ , taking maximum for all elements of the left hand side and maximum for all columns of the right hand side, we obtain the following recursive inequality,

$$\max |\tilde{A}_{-\ell,-\ell}^{(t+1)} \tilde{A}_{-\ell,-\ell}^{(t)} \cdots \tilde{A}_{-\ell,-\ell}^{(1)}| \leq (1 - \eta) \max |\tilde{A}_{-\ell,-\ell}^{(t)} \cdots \tilde{A}_{-\ell,-\ell}^{(1)}|, \quad t = 1, \dots, T - 1.$$

With  $\max |\tilde{A}_{-\ell,-\ell}^{(1)}| \leq 1 - \eta$ , multiplying all the recursive inequalities in terms of  $t = 1, 2, \dots, T - 1$ , we have

$$\max \left| \prod_{t=1}^T \tilde{A}_{-\ell,-\ell}^{(t)} \right| \leq (1 - \eta)^T.$$

For the rest factor  $\tilde{A}_{-\ell,-\ell}^{(-1)}$ , since its row sum is no larger than 1, we can similarly obtain

$$\max \left| \tilde{A}_{-\ell,-\ell}^{(-1)} \prod_{t=1}^T \tilde{A}_{-\ell,-\ell}^{(t)} \right| \leq \max \left| \prod_{t=1}^T \tilde{A}_{-\ell,-\ell}^{(t)} \right| \leq (1 - \eta)^T.$$

Hence, continuing (27), we have

$$\begin{aligned} \|W_{-\ell,\ell}^{(k)} - n^{-1}\mathbf{1}_{n-1}\|_2 &\leq \frac{1}{\sqrt{n}} \left\| \prod_{i=0}^{k-1} A_{-\ell,-\ell}^{(i)} \right\|_F \leq \sqrt{n} \max \left| \prod_{i=1}^{k-1} A_{-\ell,-\ell}^{(i)} \right| \\ &\leq \sqrt{n} \max \left| \tilde{A}_{-\ell,-\ell}^{(-1)} \prod_{t=1}^T \tilde{A}_{-\ell,-\ell}^{(t)} \right| \leq \sqrt{n} (1 - \eta)^T. \end{aligned}$$

Knowing that  $W_{\ell,\ell}^{(k)} - n^{-1} \equiv 0$ , we have  $\|M_{-\ell,\ell}^{(k)} - n^{-1}\mathbf{1}_{n-1}\|_2 = \|M_{\cdot,\ell}^{(k)} - n^{-1}\mathbf{1}_n\|_2$ . Taking all columns of  $W^{(k)}$  into consideration, we finally have

$$\|W^{(k)} - E_n\|_F \leq n(1 - \eta)^T.$$

Without loss of generality, we let  $k > B$ , so that  $T = \lfloor k/B \rfloor \geq k/B - 1$ . So the convergence rate can be bounded as

$$\|W^{(k)} - E_n\|_F \leq \frac{n}{1 - \eta} \left( \sqrt[B]{1 - \eta} \right)^k.$$

**Proof of (iii).** Using the iteration equation (8), we can bound the consensus error  $\|\mathbf{z}^{(k)} - E_n \mathbf{x}\|_F$  as

$$\begin{aligned} \|\mathbf{z}^{(k)} - E_n \mathbf{x}\|_F &= \|W^{(k)} \mathbf{x} - E_n \mathbf{x}\|_F \leq \|W^{(k)} - E_n\|_F \|\mathbf{x}\|_F \\ &\leq \frac{n}{1 - \eta} \left( \sqrt[B]{1 - \eta} \right)^k \|\mathbf{x}\|_F, \end{aligned}$$

which finishes the proof.  $\square$

## A.6 Proof of Lemma 1

*Proof.* Consider the update of  $\bar{x}^{(k+1)}$  using (13):

$$\begin{aligned} \bar{x}^{(k+1)} &= n^{-1} \mathbf{1}_n^\top (A^{(k)} \mathbf{x}^{(k)} - \gamma W^{(k)} \mathbf{g}^{(k)}) \\ &= \bar{x}^{(k)} - \gamma \bar{g}^{(k)} + \underbrace{n^{-1} \mathbf{1}_n^\top (A^{(k)} - E_n) \Delta_x^{(k)}}_{\text{Consensus Error}} - \underbrace{n^{-1} \gamma \mathbf{1}_n^\top (W^{(k)} - E_n) \mathbf{g}^{(k)}}_{\text{Descent Deviation}} \end{aligned}$$

We apply the  $L$ -smooth inequality on  $\bar{x}^{(k+1)}$ ,  $\bar{x}^{(k)}$  and using average inequality:

$$\begin{aligned} f(\bar{x}^{(k+1)}) &\leq f(\bar{x}^{(k)}) - \gamma \langle \bar{g}^{(k)}, \nabla f(\bar{x}^{(k)}) \rangle \\ &\quad + n^{-1} \langle \mathbf{1}_n^\top (A^{(k)} - E_n) \Delta_x^{(k)}, \nabla f(\bar{x}^{(k)}) \rangle \\ &\quad - n^{-1} \gamma \langle \mathbf{1}_n^\top (W^{(k)} - E_n) \mathbf{g}^{(k)}, \nabla f(\bar{x}^{(k)}) \rangle + \frac{3\gamma^2 L}{2} \|\bar{g}^{(k)}\|^2 \\ &\quad + \frac{3L}{2n^2} \|\mathbf{1}_n^\top (A^{(k)} - E_n) \Delta_x^{(k)}\|^2 + \frac{3\gamma^2 L}{2n^2} \|\mathbf{1}_n^\top (W^{(k)} - E_n) \mathbf{g}^{(k)}\|^2 \end{aligned} \tag{28}$$

To proceed on, we split the right-hand side into 5 terms, which are

$$\begin{aligned} \Delta_1^{(k)} &:= -\gamma \langle \bar{g}^{(k)}, \nabla f(\bar{x}^{(k)}) \rangle + \frac{3\gamma^2 L}{2} \|\bar{g}^{(k)}\|^2, \\ \Delta_2^{(k)} &:= n^{-1} \langle \mathbf{1}_n^\top (A^{(k)} - E_n) \Delta_x^{(k)}, \nabla f(\bar{x}^{(k)}) \rangle, \\ \Delta_3^{(k)} &:= -n^{-1} \gamma \langle \mathbf{1}_n^\top (W^{(k)} - E_n) \mathbf{g}^{(k)}, \nabla f(\bar{x}^{(k)}) \rangle, \\ \Delta_4^{(k)} &:= \frac{3L}{2n^2} \|\mathbf{1}_n^\top (A^{(k)} - E_n) \Delta_x^{(k)}\|^2, \quad \Delta_5^{(k)} := \frac{3\gamma^2 L}{2n^2} \|\mathbf{1}_n^\top (W^{(k)} - E_n) \mathbf{g}^{(k)}\|^2. \end{aligned}$$

When  $\gamma \leq \frac{1}{6L}$ , the first term can be bounded as:

$$\Delta_1^{(k)} = -\frac{\gamma - 3\gamma^2 L}{2} \|\bar{g}^{(k)}\|^2 - \frac{\gamma}{2} \|\nabla f(\bar{x}^{(k)})\|^2 + \frac{\gamma}{2} \|\bar{g}^{(k)} - \nabla f(\bar{x}^{(k)})\|^2$$

$$\leq -\frac{\gamma}{4}\|\bar{g}^{(k)}\|^2 - \frac{\gamma}{2}\|\nabla f(\bar{x}^{(k)})\|^2 + \frac{\gamma L^2}{2n}\|\Delta_x^{(k)}\|_F^2$$

For the second term, we have the observation: For any  $y \in \mathbb{R}^n$ ,  $\bar{y} := n^{-1}\mathbf{1}_n^\top y$  represents the average of all its elements, while  $\tilde{y} := n^{-1}\mathbf{1}_n^\top A^{(k)}y$  is a convex but not necessarily average combination of all its elements. But the following inequality always holds:  $(\tilde{y} - \bar{y})^2 \leq \max_i |y_i - \bar{y}|^2 \leq \sum_{i=1}^n (y_i - \bar{y})^2$ . Generalizing to  $d$  columns, we have  $\|n^{-1}\mathbf{1}_n^\top (A^{(k)} - E_n)\mathbf{y}\|^2 \leq \|\mathbf{y} - E_n\mathbf{y}\|_F^2$ . And we further have  $\Delta_x^{(k)} - E_n\Delta_x^{(k)} = \Delta_x^{(k)}$ . Hence, using Cauchy-Schwarz inequality,  $\Delta_2^{(k)}$  can be bounded as:

$$\begin{aligned} \Delta_2^{(k)} &\leq \|n^{-1}\mathbf{1}_n^\top (A^{(k)} - E_n)\Delta_x^{(k)}\| \cdot \|\nabla f(\bar{x}^{(k)})\| \\ &\leq \|\Delta_x^{(k)}\|_F \cdot \|\nabla f(\bar{x}^{(k)})\| \leq \frac{p_k}{2}\|\Delta_x^{(k)}\|_F^2 + \frac{1}{2p_k}\|\nabla f(\bar{x}^{(k)})\|^2, \end{aligned}$$

where the parameter  $p_k$  is to be determined.

Similarly, the third term can be bounded as:

$$\begin{aligned} \Delta_3^{(k)} &\leq \gamma\|n^{-1}\mathbf{1}_n^\top (W^{(k)} - E_n)\mathbf{g}^{(k)}\| \cdot \|\nabla f(\bar{x}^{(k)})\| \\ &\leq \gamma n^{-1/2}\|W^{(k)} - E_n\|_F \|\mathbf{g}^{(k)}\|_F \|\nabla f(\bar{x}^{(k)})\| \\ &\leq \gamma \frac{C_W \beta^{R_k}}{\sqrt{n}} \left( \frac{q_k}{2} \|\mathbf{g}^{(k)}\|_F^2 + \frac{1}{2q_k} \|\nabla f(\bar{x}^{(k)})\|^2 \right), \end{aligned}$$

where the third inequality uses (9), and  $q_k$  is a constant to be determined.

The fourth term is smaller than  $\frac{3L}{2}\|\Delta_x^{(k)}\|^2$ , and the fifth term is smaller than  $\frac{3C_W^2 \gamma^2 L \beta^{2R_k}}{2n} \|\mathbf{g}^{(k)}\|_F^2$ . Now combine these estimates and plug them into (28), we obtain that

$$\begin{aligned} &\frac{\gamma}{4}\|\bar{g}^{(k)}\|^2 + \left( \frac{\gamma}{2} - \frac{1}{2p_k} - \frac{C_W \beta^{R_k} \gamma}{2q_k \sqrt{n}} \right) \|\nabla f(\bar{x}^{(k)})\|^2 \\ &\leq f(\bar{x}^{(k)}) - f(\bar{x}^{(k+1)}) + \left( \frac{\gamma L^2}{2n} + \frac{p_k}{2} + \frac{3L}{2} \right) \|\Delta_x^{(k)}\|_F^2 \\ &\quad + \left( \frac{\gamma C_W \beta^{R_k} q_k}{2\sqrt{n}} + \frac{3C_W^2 \gamma^2 L \beta^{2R_k}}{2n} \right) \|\mathbf{g}^{(k)}\|_F^2. \end{aligned}$$

Selecting  $q_k = \frac{3C_W \beta^{R_k}}{\sqrt{n}}$ ,  $p_k = \frac{3}{\gamma}$ , we obtain that

$$\begin{aligned} &\frac{\gamma}{4}\|\bar{g}^{(k)}\|^2 + \frac{\gamma}{6}\|\nabla f(\bar{x}^{(k)})\|^2 \\ &\leq f(\bar{x}^{(k)}) - f(\bar{x}^{(k+1)}) + \left( \frac{\gamma L^2}{2n} + \frac{3}{2\gamma} + \frac{3L}{2} \right) \|\Delta_x^{(k)}\|_F^2 + \frac{3\gamma(1 + \gamma L)C_W^2 \beta^{2R_k}}{2n} \|\mathbf{g}^{(k)}\|_F^2. \end{aligned}$$

By taking  $\gamma \leq \frac{1}{6L}$ , we obtain that

$$\begin{aligned} &\frac{\gamma}{4}\|\bar{g}^{(k)}\|^2 + \frac{\gamma}{6}\|\nabla f(\bar{x}^{(k)})\|^2 \\ &\leq f(\bar{x}^{(k)}) - f(\bar{x}^{(k+1)}) + \frac{127}{72\gamma} \|\Delta_x^{(k)}\|_F^2 + \frac{2\gamma C_W^2 \beta^{2R_k}}{n} \|\mathbf{g}^{(k)}\|_F^2. \end{aligned} \tag{29}$$

Finally, to deal with the stacked gradient term  $\|\mathbf{g}^{(k)}\|_F^2$ , with  $L$ -smooth assumption, we know that  $\forall x, y \in \mathbb{R}^d, i \in [n]$ ,

$$f_i(y) \leq f_i(x) + \langle \nabla f_i(x), y - x \rangle + \frac{L}{2} \|y - x\|^2.$$

By taking  $y = x - \frac{1}{L}\nabla f_i(x)$ , we obtain that  $\frac{1}{2L}\|\nabla f_i(x)\|^2 \leq f_i(x) - f_i(y) \leq f_i(x) - f_i^*$ . Furthermore, using  $L$ -smoothness property and Cauchy-Schwarz inequality, we have

$$\begin{aligned}
\|\mathbf{g}^{(k)}\|_F^2 &= \|\nabla F(\mathbf{x}^{(k)})\|_F^2 \leq 2\|\nabla F(\mathbf{x}^{(k)}) - \nabla F(E_n \mathbf{x}^{(k)})\|_F^2 + 2\|\nabla F(E_n \mathbf{x}^{(k)})\|_F^2 \\
&= 2\sum_{i=1}^n \|\nabla f_i(x_i^{(k)}) - \nabla f_i(\bar{x}^{(k)})\|^2 + 2\sum_{i=1}^n \|\nabla f_i(\bar{x}^{(k)})\|^2 \\
&\leq 2L^2\sum_{i=1}^n \|x_i^{(k)} - \bar{x}^{(k)}\|^2 + 4L\sum_{i=1}^n (f_i(\bar{x}^{(k)}) - f_i^*) \\
&= 2L^2\|\Delta_x^{(k)}\|_F^2 + 4nL(f(\bar{x}^{(k)}) - f^*),
\end{aligned} \tag{30}$$

where  $f^* := n^{-1}\sum_{i=1}^n f_i^*$ . To further simplify the inequality, we require  $R_k \geq \ln(C_W)/\ln(1/\beta)$  to ensure  $C_W\beta^{R_k} \leq 1$ . Substituting  $\|\mathbf{g}^{(k)}\|_F^2$  with (30) into (29) and using  $\gamma \leq \frac{1}{6L}$ , we obtain the conclusion.  $\square$

## A.7 Proof of Lemma 2

*Proof.* Recall the update format (13) with simplified notations:

$$\mathbf{x}^{(k+1)} = A^{(k)}\mathbf{x}^{(k)} - \gamma W^{(k)}\mathbf{g}^{(k)}. \tag{31}$$

Based on the  $R_k$ -length list  $\{A^{(k,r)}\}_{r=0}^{R_k-1}$ , by adding the remainder row-stochastic matrices arbitrarily, we obtain the sequence  $\{A^{(k,r)}\}_{r=0}^\infty$  satisfying Proposition 2, and denote the corresponding limit as  $A_\infty^{(k)} = \mathbb{1}_n \pi^{(k)}$ . Left-multiply  $(I - E_n)$  on both sides of (31) and we obtain that

$$\Delta_x^{(k+1)} = (I - E_n)(A^{(k)} - A_\infty^{(k)})\Delta_x^{(k)} - \gamma(I - E_n)(W^{(k)} - E_n)\mathbf{g}^{(k)}. \tag{32}$$

Therefore, we can apply the Cauchy-Schwarz inequality on (32) and obtain that

$$\begin{aligned}
\|\Delta_x^{(k+1)}\|_F^2 &\leq 2\|(I - E_n)(A^{(k)} - A_\infty^{(k)})\Delta_x^{(k)}\|_F^2 + 2\gamma^2\|(I - E_n)(W^{(k)} - E_n)\mathbf{g}^{(k)}\|_F^2 \\
&\leq 2\|A^{(k)} - A_\infty^{(k)}\|_F^2\|\Delta_x^{(k)}\|_F^2 + 2\gamma^2\|W^{(k)} - E_n\|_F^2\|\mathbf{g}^{(k)}\|_F^2 \\
&\leq 2C_A^2\beta^{2R_k}\|\Delta_x^{(k)}\|_F^2 + 2\gamma^2C_W^2\beta^{2R_k}\|\mathbf{g}^{(k)}\|_F^2 \\
&\leq (2C_A^2\beta^{2R_k} + 4\gamma^2L^2C_W^2\beta^{2R_k})\|\Delta_x^{(k)}\|_F^2 + 8n\gamma^2LC_W^2\beta^{2R_k}(f(\bar{x}^{(k)}) - f^*),
\end{aligned}$$

where the second inequality is due to  $\|I_n - E_n\|_2 = 1$ , the third inequality uses the linear convergence rate in (5) and (9), and the last inequality is from (30). Choose  $R_k \geq \max\{\ln(C_W)/\ln(1/\beta), \ln(3C_A)/\ln(1/\beta)\}$  and  $\gamma \leq \frac{1}{6L}$  to bound the coefficient of  $\|\Delta_x^{(k)}\|_F^2$  and the conclusion follows.  $\square$

## A.8 Proof of Lemma 3

*Proof.* Define  $u_k := 1 + \frac{c}{(1+k)^2}$ ,  $U_k = \prod_{l=0}^k u_l$ , and  $U_{-1} := 1$  for convenience, which imply  $u_k = U_k/U_{k-1}, \forall k \geq 0$ . Then (17) can be transformed as

$$U_k^{-1}S_k \leq U_{k-1}^{-1}D_k - U_k^{-1}D_{k+1} + U_k^{-1}F_k, \quad \forall k \geq 0. \tag{33}$$

Since  $u_k \geq 1, \forall k \geq 0$ ,  $U_k$  is monotonically increasing. Therefore, summing (33) from  $k = 0$  to  $K - 1$  and telescoping, we have

$$U_{K-1}^{-1} \sum_{k=0}^{K-1} S_k \leq \sum_{k=0}^{K-1} U_k^{-1} S_k \leq D_0 - U_{K-1}^{-1} D_K + \sum_{k=0}^{K-1} U_k^{-1} F_k \leq D_0 + U_0^{-1} \sum_{k=0}^{K-1} F_k.$$

On one hand,  $U_0 = u_0 = 1 + c$ . On the other hand,

$$\begin{aligned} U_{K-1} &= \prod_{k=0}^{K-1} \left(1 + \frac{c}{(1+k)^2}\right) = \exp\left(\sum_{k=0}^{K-1} \ln\left(1 + \frac{c}{(1+k)^2}\right)\right) \\ &\leq \exp\left(\sum_{k=0}^{K-1} \frac{c}{(1+k)^2}\right) \leq \exp(2c). \end{aligned}$$

Substitute  $U_0$  with its value and  $U_{K-1}$  with its upper bound and we have the conclusion.  $\square$

## A.9 Proof of Theorem 2

*Proof.* Based on Lemma 1, 2 and 3, we obtain the inequality (19). As Algorithm 3 is initialized at consensus, namely  $\Delta_x^{(0)} = 0$ , the terms  $\sum_{k=1}^{K-1} \|\Delta_x^{(k)}\|_F^2$  and  $\sum_{k=0}^{K-1} \|\Delta_x^{(k)}\|_F^2$  on both sides are canceled. The non-negative terms  $\sum_{k=0}^{K-1} \|\bar{g}^{(k)}\|^2$  and  $\|\Delta_x^{(K)}\|_F^2$  can be directly omitted. And then the main inequality (20) follows. The choice of step size  $\gamma$  and the inner iteration rounds  $R_k$  are determined by Lemma 1, 2, and the sufficient choice when utilizing Lemma 3.  $\square$

# B Experiment Details and Supplementary Experiments

## B.1 Settings of Network Topology

Throughout our experiments, all the network topologies can be classified into two categories. The one contains purely random networks, and the other contains fixed latent topologies with possibilities of disconnection. For purely random networks, we only need a communication probability  $p_c$ , and each node  $i$  is expected to send information to each node  $j$  in each time interval  $k$  with probability  $p_c$ . For networks with a latent topology, we first need a strongly connected directed network, which can be ring topology or a strongly connected directed network with a given sparsity rate. Next, each edge of the latent network can disappear in each time interval  $k$  with a probability  $p_d$ . Note that the disconnections are reflected in out-degrees. This also produces a series of time-varying topologies.

In the experiments comparing PUSH-SUM/ PUSH-DIGING with PULM / PULM-DGD, we also considered the packet loss probability  $p_t$  after transmission, before reception. This case is different from the case stated before where  $p_d$  of disconnections occur, as packet losses cannot be anticipated before sending messages and are not reflected in out-degrees, which PUSH-SUM/ PUSH-DIGING cannot capture.

## B.2 Settings of Consensus Problem

Consensus problem is to reach the average of a series of vectors  $x_1, x_2, \dots, x_n \in \mathbb{R}^d$ . Algorithm 2 together with PUSH-SUM [9] are designed to solve the consensus problem. To test the effectiveness of Algorithm 2, we define the following error metric

$$e^{(k)} := \frac{\|\mathbf{z}^{(k)} - \bar{\mathbf{x}}\|_F}{\|\mathbf{x} - \bar{\mathbf{x}}\|_F}, \quad (34)$$

where  $\mathbf{z}^{(k)}$ ,  $\mathbf{x}$  are defined in Algorithm 2 and  $\bar{\mathbf{x}} := E_n \mathbf{x}$ .

## B.3 Settings of Logistic Regression

Logistic regression problem considers dataset  $\{x_s, y_s\}_{s=1}^S$ , where  $x_s \in \mathbb{R}^d$ ,  $y_s \in \{+1, -1\}$ ,  $S$  is the number of total samples. In distributed context, we divide the dataset into  $n$  sub-datasets  $\{x_{i,s}, y_{i,s}\}_{s=1}^{S_i}$ ,  $i = 1, 2, \dots, n$ . And for each node with a local sub-dataset, we define the local objective function as

$$f_i(w, b) := \frac{1}{S_i} \sum_{i=1}^{S_i} \log \left( 1 + \exp \left( -y_{i,s} (x_{i,s}^\top w + b) \right) \right) + \lambda \left( \frac{b^2}{1 + b^2} + \sum_{j=1}^d \frac{w_j^2}{1 + w_j^2} \right),$$

where  $w_j$  indicates the  $j$ -th element of vector  $w \in \mathbb{R}^d$ ,  $\lambda$  is the penalty parameter which controls the proportion of the non-convex penalty term. Throughout our experiments, we always chose  $\lambda = 0.1$ . Finally, we define the global objective function  $f(w, b) := \frac{1}{n} \sum_{i=1}^n f_i(w, b)$ .

For experiments with synthetic data, we use the following data generation strategy: 1. Randomly choose global latent weight and bias  $w^*, b^*$ . 2. Given a heterogeneity coefficient  $\sigma_h \geq 0$ , generate each local latent weight and bias  $w_i^*, b_i^*$  by sampling  $w_i^* \sim \mathcal{N}(w^*, \sigma_h^2 I_d)$ ,  $b_i^* \sim \mathcal{N}(b^*, \sigma_h^2)$ . 3. For each sample  $s$  of each node  $i$ , randomly generate  $x_{i,s}$ , and compute  $p_{i,s} = \sigma(x_{i,s}^\top w_i^* + b_i^*)$ , where  $\sigma(x) := 1/(1 + e^{-x})$  is the sigmoid function. Then determine  $y_{i,s} = +1$  with probability  $p_{i,s}$  and  $y_{i,s} = -1$  with probability  $1 - p_{i,s}$ .

In our experiments of logistic regression with synthetic data, we chose  $n = 10, d = 30, S = 1000, \sigma_h = 0.1$ . For experiments with real data, we choose the UCI machine learning dataset ‘‘Human Activity Recognition Using Smartphones<sup>2</sup>’’. We divided the dataset into 10 subsets, and chose the class id 1 as the response variable.

## B.4 Settings of MNIST and CIFAR-10 Classification

The training of MNIST dataset was conducted on the LeNet neural network model; and meanwhile we chose ResNet-18 to handle the training of CIFAR-10 dataset. The training dataset can be divided either randomly or by labels. Dividing dataset by labels means arranging samples into ten nodes according to their ground truth label from 0 to 9. Throughout our all experiments on MNIST and CIFAR-10, we set the batch-size  $b = 100$ .

<sup>2</sup><https://archive.ics.uci.edu/dataset/240/human+activity+recognition+using+smartphones>

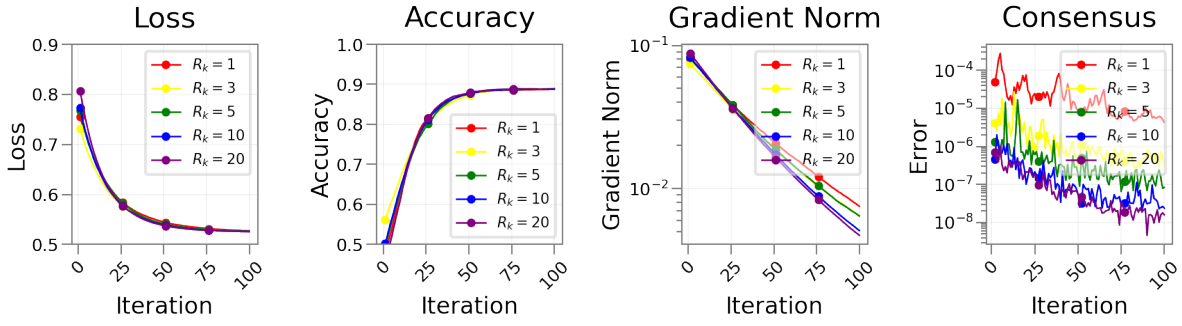


Figure A1: Effect of communication rounds  $R_k$  in logistic regression with synthetic data

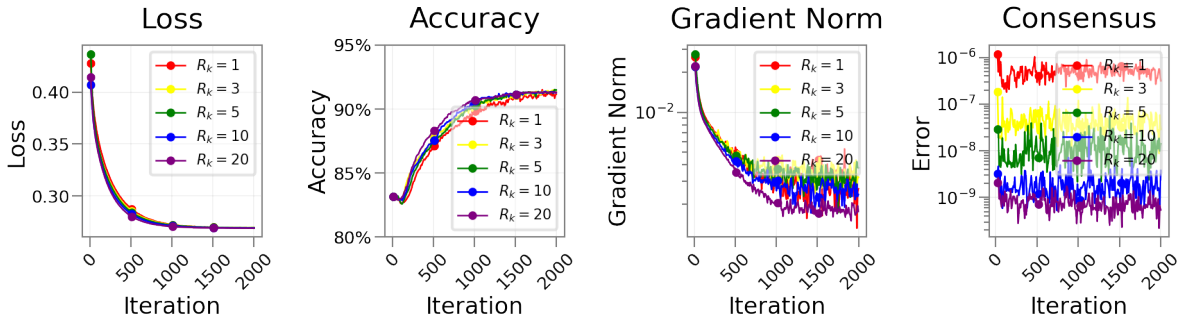


Figure A2: Effect of communication rounds  $R_k$  in logistic regression with real data

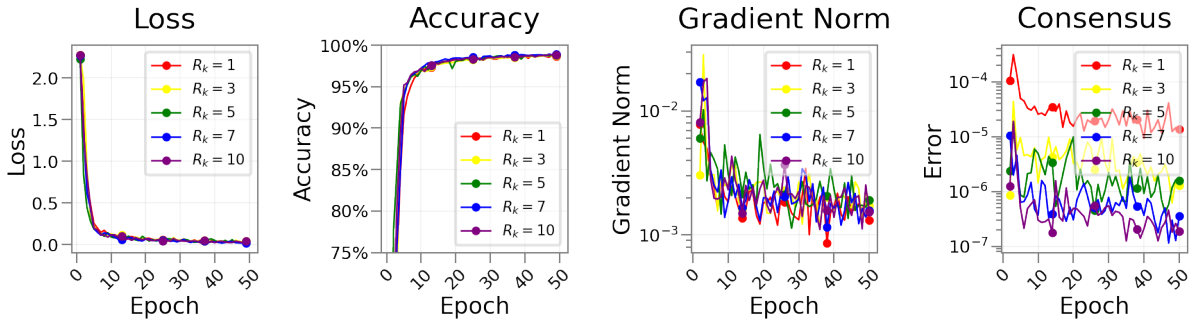


Figure A3: Effect of communication rounds  $R_k$  in MNIST training

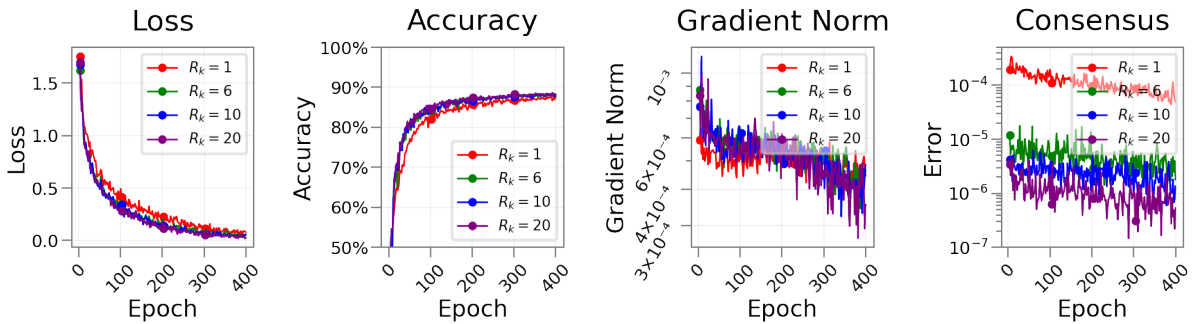


Figure A4: Effect of communication rounds  $R_k$  in CIFAR-10 training

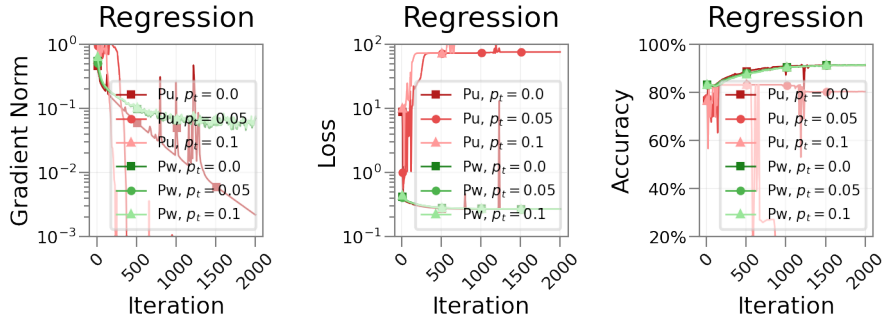


Figure A5: Comparison with Push-DIGing on real dataset

## B.5 Details of Experiments Concerned with Different Inner Communication Rounds $R_k$

Figures A1, A2, A3, A4 show the detailed results of experiments corresponding to Section 5.2. For all the four sets of experiments, we chose the time-varying topologies with a fixed latent strongly connected network, whose sparsity  $s = 0.3$ , but suffered a disconnection rate  $p_d = 0.4$ . We allocated samples randomly into 10 nodes for MNIST and CIFAR-10 training. Except for the logistic regression on the real dataset which used a learning rate of 0.01, the rest of the problems all used a learning rate of 0.1.

We defined the following metric to indicate the consensus error among all nodes:

$$e^{(k)} := \sqrt{\frac{1}{d} \sum_{j=1}^d \left( \frac{1}{n} \sum_{i=1}^n (x_{i,j}^{(k)} - \bar{x}_j^{(k)})^2 \right)},$$

where  $\bar{x}_j^{(k)} := \frac{1}{n} \sum_{i=1}^n x_{i,j}^{(k)}$ . It can be noticed that the consensus error decreases as the rounds of inner communications increase, but not linearly. The contribution of the rounds of communications to error reduction become less obvious as the rounds increase. And for most non-convex problems, the consensus error is not decisive.

## B.6 Supplementary Experiments: Comparison with Push-DIGing on Real Dataset

To further illustrate the effectiveness of our algorithm compared with Push-DIGing, we also conducted experiments of logistic regression on real dataset for comparison. The other settings were identical to those in Section 5.1, while the learning rate was set as 0.01 for the convergence on real dataset. The results are demonstrated in Figure A5. And the conclusion is the same as in Section 5.1.

## B.7 Supplementary Experiments: Performances on Different Topologies

To examine the effectiveness of our algorithms, we further conducted experiments on different topologies.

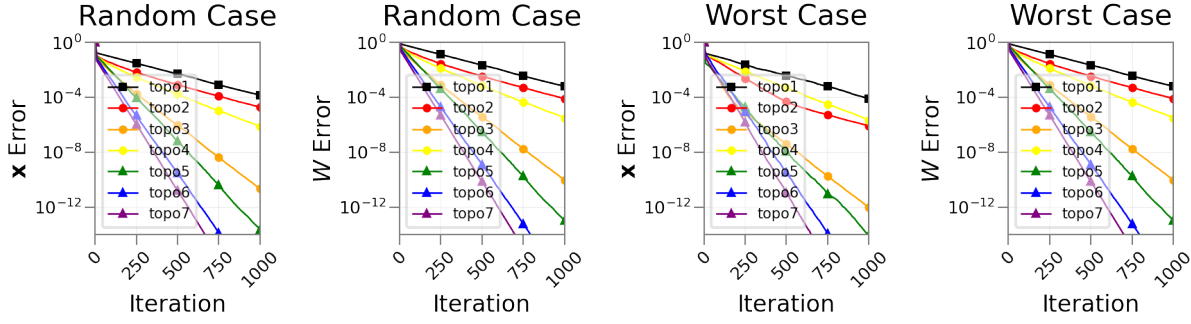


Figure A6: Consensus problems on different topologies

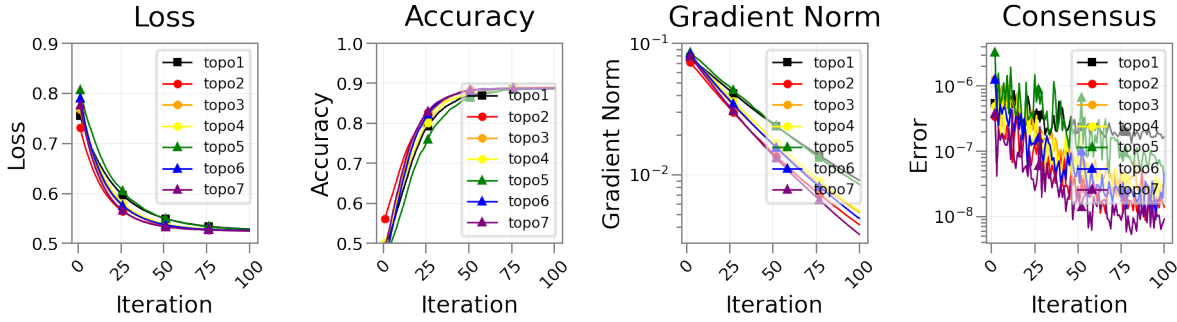


Figure A7: Logistic regression with synthetic data on different topologies

Figure A6 shows the performance of Algorithm 2 on different topologies. The number of nodes was 20, and the seven topologies we chose were respectively: topo 1, ring topo with disconnection rate 0.2; topo 2, fixed latent topo of sparsity 0.2, with disconnection rate 0.2; topo 3, fixed latent topo of sparsity 0.3, with disconnection rate 0.2; topo 4, fixed latent topo of sparsity 0.3, with disconnection rate 0.4; topo 5, random topo with connection rate 0.1; topo 6, random topo with connection rate 0.2; topo 7, random topo with connection rate 0.3. For the data to be averaged, we considered two cases. The one used randomly generated data; while the other generated  $n - 1$  data randomly, but the last one significantly far from the cluster of the other nodes, which was to some degree a worst case. The metric to measure error of  $\mathbf{x}$  is defined in (34), and we were also interested in the error of  $W^{(k)}$ , namely  $\|W^{(k)} - E_n\|_F$ .

Based on the results, we can draw two main conclusions: Algorithm 2 is robust dealing with different cases to be averaged, as it performed similarly in random and worst cases. Besides, purely random topologies own better convergence properties than topologies with a fixed latent network, as purely random topologies may have a smaller  $B$  or larger  $\eta$  defined in Proposition 1.

Figure A7 and A8 show the results of Algorithm 3 on logistic regression problem using synthetic data and real data respectively. The seven topologies used for them were identical to those in Figure A6. The inner communication rounds  $R_k$  were always 10. Learning rates were 0.1 for synthetic dataset and 0.01 for real

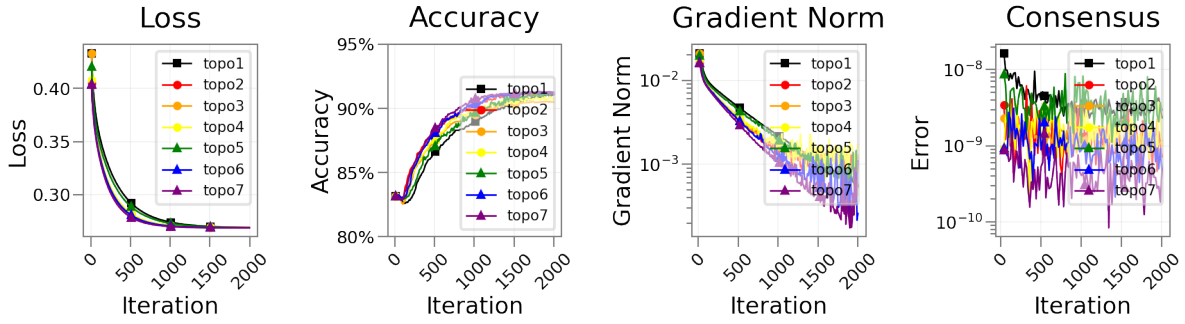


Figure A8: Logistic regression with real data on different topologies

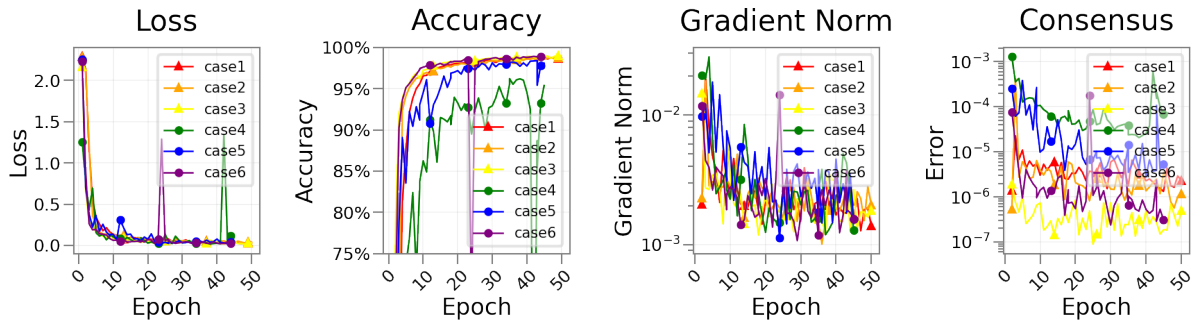


Figure A9: MNIST training on different topologies

dataset. Consistent with the former experiments, topologies owning a better convergence property led to a smaller consensus error. But on the other hand, a rough accuracy of consensus is sufficient for non-convex problems, when better consensus brings no significant benefits.

Figure A9 shows the results of Algorithm 3 on MNIST training. Learning rate was set as 0.1. There were six cases which we considered: case1, random data distribution on ring latent topology; case2, random data distribution on fixed latent topology; case3, random data distribution on random topologies; case4, label-based distribution on ring latent topology; case5, label-based distribution on fixed latent topology; case6, label-based distribution on random topologies. Data were always distributed into ten nodes, and the two data distribution strategies can be referred to Section B.4. The three topology types used were: ring latent topology with a disconnection rate 0.2; fixed latent topology with sparsity 0.3 and with a disconnection rate 0.4; random topologies with connection rate 0.3. When allocating data by their labels, we should notice that different nodes might not own the same number of data. Hence, the process of epochs among different nodes might not be synchronous. We took the number of epochs within the slowest node as the indicator of the global number of epochs. Based on the results, we draw the conclusion that the properties of topologies and the distribution strategies of dataset play a more important role in the convergence of the whole problem than the inner communication rounds. However, in fairly mild settings, Algorithm 3 is still able to show good performance without a large overhead of communication or computation.